CHALMERS
UNIVERSITY OF TECHNOLOGY

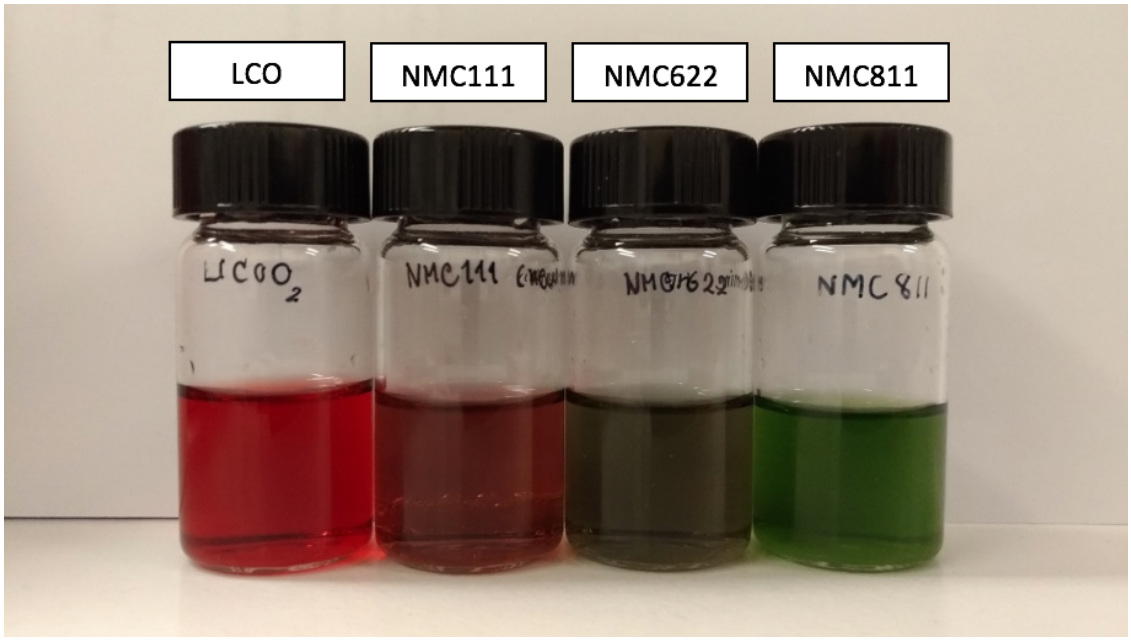

Recycling of lithium-ion batteries

Determination of optimal parameters for the application of hydrogen peroxide as reducing agent in the leaching process

Master's thesis in Innovative and Sustainable Chemical Engineering

PIAMCHEEWA BENJAMASUTIN
RAKSINA PROMPHAN

Department of Chemistry & Chemical Engineering
CHALMERS UNIVERSITY OF TECHNOLOGY
Gothenburg, Sweden 2020

Master's thesis 2020

Recycling of lithium-ion batteries

Determination of optimal parameters for the application of hydrogen peroxide as reducing agent in the leaching process

PIAMCHEEWA BENJAMASUTIN

RAKSINA PROMPHAN

CHALMERS
UNIVERSITY OF TECHNOLOGY

Department of Chemistry and Chemical Engineering
Division of Industrial Materials Recycling
Chalmers University of Technology
Gothenburg, Sweden 2020

Recycling of lithium-ion batteries
Determination of optimal parameters for the application of hydrogen peroxide as reducing agent in the leaching process
PIAMCHEEWA BENJAMASUTIN and RAKSINA PROMPHAN

Supervisor: Dr. Martina Petranikova, Chalmers
Supervisor: Dr. Magnus Paulsson, Nouryon
Examiner: Professor Britt-Marie Steenari, Chalmers

Master's Thesis 2020
Department of Chemistry and Chemical Engineering
Division of Industrial Materials Recycling
Chalmers University of Technology
SE-412 96 Gothenburg
Telephone +46 31 772 1000

A collaboration with Nouryon Pulp and Performance Chemicals AB

Cover: Sulfuric acid leaching solution containing hydrogen peroxide for four cathode materials which are LCO, NMC111, NMC622, and NMC811.

Recycling of lithium-ion batteries:
Determination of optimal parameters for the application of hydrogen peroxide as reducing agent in the leaching process

PIAMCHEEWA BENJAMASUTIN and RAKSINA PROMPHAN
Department of Chemistry and Chemical Engineering
Chalmers University of Technology

Abstract

The use of secondary Li-ion batteries has grown significantly in recent years because of their high energy density and are currently used in a wide range of applications such as electronic appliances, energy storage applications, and electric vehicles. Due to the limited resources and environmental problems after end-of-use, the recycling of valuable metals from spent batteries is substantially essential. In this work, sulfuric acid (H_2SO_4) leaching with the help of a reducing agent (hydrogen peroxide) of four different cathode materials was studied. The cathode materials that were investigated are LCO, NMC111, NMC622, and NMC811. The aim was to determine the optimal leaching conditions including leaching temperature, acid concentration, solid-to-liquid ratio, amount (%v/v), and addition strategy of the reducing agent. The optimal leaching temperature and acid concentration, without the addition of hydrogen peroxide and current collectors, were 50°C and 2 M H_2SO_4, respectively. A solid-to-liquid ratio of 1:20 g/mL was selected for further leaching experiments carried out when hydrogen peroxide was added as a reducing agent. In addition, a better mixing was found to promote the leaching performance. Both metals' leaching efficiencies for cobalt, lithium, nickel, and manganese and the hydrogen peroxide consumption were determined in order to determine the optimal hydrogen peroxide concentration in the leaching solution and the best way to add hydrogen peroxide. Different amounts of hydrogen peroxide were needed to efficiently leach the four different cathode materials studied. Addition of hydrogen peroxide once at the beginning of leaching yielded 100% leaching efficiency faster than adding hydrogen peroxide at several occasions (same total hydrogen peroxide charge). Moreover, an addition of copper and aluminum foils, which represent the current collectors that also can act as reducing agents, can improve all metal leaching efficiencies except for lithium because lithium doesn't need to change oxidation state. It was thus shown that the proposed leaching conditions can effectively leach valuable metals out from pure cathode materials. Crushed spent cathode material ("black mass") with the composition of $Li_{1.087}Ni_{0.308}Mn_{0.300}Co_{0.392}O_2$ was then leached with the optimum conditions for pure cathode material (NMC111). The outcome was a leaching efficiency of almost 100% for cobalt, nickel, and manganese and with low amounts of residual hydrogen peroxide in the leachate.

Keywords: Sulfuric acid leaching, hydrometallurgical recycling, Li-ion batteries, LCO, NMC, hydrogen peroxide, leaching efficiency.

Acknowledgements

First and foremost, we would like to appreciatingly express our gratitude toward our supervisor, Dr. Martina Petranikova, for giving us an opportunity to do this interesting thesis on the topic of recycling Li-ion batteries. Also with her kind support, patience and immense knowledge helped us all the time doing our master's thesis work: performing experiment and writing this report. We could not imagined to have a better supervisor for our research.

Beside our supervisor, we also would like to extend our gratitude to Dr. Magnus Paulsson and Ph.Lic. Pia Hellström from Nouryon Pulp and Performance Chemicals AB for being our advisors, providing us knowledge about chemistry of hydrogen peroxide, kind support of such substance and very useful recommendations.

We would like to thank Britt-Marie Steenari, our examiner, for letting us to do this thesis.

Our acknowledgement also goes to our laboratory colleagues at the department of Nuclear Chemistry/Industrial Material Recycling for giving advice and recommendations. Also giving thanks to Luis Guillermo Gonzalez Fonseca and Stellan Holgersson for the help with ICP-OES and Nathalia Cristine Vieceli for her assist on analyzing the component of spent Li-ion batteries.

Piamcheewa Benjamasutin and Raksina Promphan, Gothenburg, June 2020

Contents

List of Figures

List of Tables

1

Introduction

Nowadays, transportation around the world predominantly relies on fossil-based fuel which is the main source of CO_2 emissions in the recent decades. The more environmentally friendly technologies are emerging from concern of environmental issues from the emission of conventional vehicles. The lithium-ion secondary batteries are crucial for many electrical devices including electric vehicles (EVs) due to their compactness and lightweight. Lithium ions have a small size that can promote the ability to intercalate in both electrodes. So, lithium-ion batteries have higher energy density compared to other types of a battery such as Nickel Cadmium (Ni-Cd) and Nickel-metal hydride (Ni-MH) [1]. An increase in demand for Li-ion batteries (LiBs) is reflected as a Compound Annual Growth Rate (CAGR). The battery's market is expected to grow approximately at a CAGR of 12.31% during 2019-2024 [2]. The mechanism and structure of a lithium-ion battery are fairly simple. There are electrochemical cells connected in series or parallel and each cell has a negative and a positive electrode which are divided by an electrolytic solution and a porous separator [3]. In the battery compartment, the electrical energy will be generated by the conversion of chemical energy via redox reactions at the cathode and anode. The working principle has two modes which are charging and discharging. There are many possible metal composition types of cathode materials for lithium ion batteries: Lithium Cobalt Oxide ($LiCoO_2$, LCO), Lithium Manganese Oxide ($LiMn_2O_4$)/Li_2MnO_3/$LiMnO_2$/Li_2MnO_2, LMO), Lithium Iron Phosphate ($LiFePO_4$, LFP), Lithium Nickel Cobalt Aluminum Oxide ($LiNiCoAlO_2$, NCA), and Lithium Nickel Manganese Cobalt Oxide ($LiNiMnCoO_2$, NMC) [4]. The strategic metal lithium is becoming an essential material for greener technology in the future. Due to the high demand of lithium for the lithium-ion batteries manufacturing, the worldwide mining production of lithium increased 13% in 2017 [5]. Although lithium is a strategic metal, the valuable metals contained in the cathode are cobalt, nickel, and to some extent manganese. In addition to lithium, cobalt is one of the main components in spent LiBs (5-20 wt.%) and as high as 25% of the cobalt produced globally is found in LiBs [6]. The EU has identified that cobalt is a critical raw material due to limited reserve and many strategic and irreplaceable industrial uses [7]. Cobalt is the most expensive metal among others as the price is 30,000 USD/MT [8]. Therefore, recovering of cobalt can definitely return benefits in terms of material depletion and economics. There are some issues with lithium-ion batteries. Since the average life cycle of the battery is relatively short, only around 10 years, several hundred thousand tons of batteries are disposed annually within EU [9, 10]. In 2017, only 46% of the batteries sold in the EU were collected for recycling and the rest undergoes inadequate disposal that can lead to environmen-

tal problems [11]. The rapid growth of battery demand also affects future battery production since lithium can be considered as a scarce natural resource and it is expected to be totally mined out by 2050. Therefore, in the near future valuable/scarce materials such as lithium, cobalt, nickel and manganese should be recycled in order to reduce the impact of raw material depletion [9].

2

Theory

2.1 Main components in batteries

The battery is an electrochemical cell that can be connected in parallel or series. Each cell contains four main components which are electrode, electrolyte, separator, and current collector. The positive and negative electrode are separated by an electrolyte that allows the transfer of positive ions from one electrode to another. According to Figure 2.1, there are two working modes that are charging and discharging. During the charging process, lithium ions will be released from the cathode to the anode via the electrolyte, free electrons will form and flow through an external circuit to a negative collector at the anode. During the discharging process, the flow of lithium ions will occur in the opposite direction. The performance of the battery depends on the battery chemistry and material of each component in the compartment. According to European Portable Battery Association (EPBA), spent LiBs (LCO chemistry) are composed of Aluminium —15-25%, Carbon, amorphous, powder —0.1-1%, Copper foil —5-15%, Diethyl Carbonate (DEC) —1-10%, Ethylene Carbonate (EC) —1-10%, Methyl Ethyl Carbonate (MEC) —1-10%, Lithium Hexafluorophosphate ($LiPF_6$) —1-5%, Graphite, powder —10-30%, Lithium Cobalt Oxide (LCO) —25-45%, Poly (vinylidene fluoride) (PVDF) —0.5-2%, steel, nickel and inert polymer [3, 12–14].

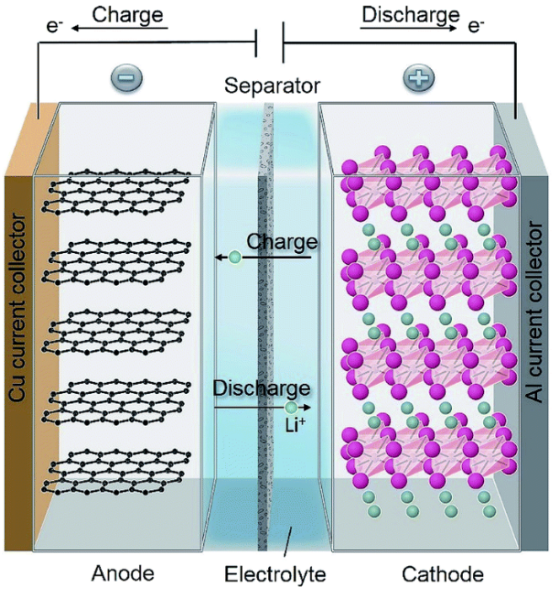

Figure 2.1: Schematic illustration of a lithium ion battery showing charge/discharge processes [15].

2.1.1 Anode

The anode is a negative electrode that tends to lose electrons and forms positive ions. The generated electrons will flow through an external circuit. There are many types of anodes that are used commercially and the anode can be composed either of carbon/graphite or non-carbon materials such as transition metal oxides [16–18]. The anode has a significant impact on improving the energy density of a lithium-ion cell, therefore the anode should fulfill the following requirements [16].

- Long cycle life.
- High rate capability and low potential against cathode material.
- High reversible gravimetric and volumetric capacity.
- The material must be low cost and environmentally friendly.

Commonly used anode materials are carbon-based graphite which has high order and micro-structure texture. Moreover, the carbonaceous material has low cost and low operational voltage which are very important factors for batteries. Those properties allow lithium to form the intercalated compound as shown in Equation 2.1 [19].

$$xM(s) + Li^{+} + e^{-} \rightleftharpoons LiM_{x}(s) \tag{2.1}$$

The graphite structure can store up to one Li^{+} for every six carbon atoms between each graphene layer. The theoretical specific capacity of graphite is 372 $mAhg^{-1}$ [20]. The ability of graphite to intercalate anions promotes the use of graphite for rechargeable batteries and graphite has excellent properties compared to other anodes.

2.1.2 Cathode

The cathode is a positive electrode comprised of active materials with different natures and is usually composed of lithium-containing materials. There are many lithium-based cathode materials that are commercialized as shown in Table 2.1, each cathode material has a different specific energy. NMC, NCA, and LFP cathode chemistries are produced in higher amounts compared to LCO, but LCO is the most common type of battery that is used in various applications, however it also has drawbacks such as a high environmental risk. The effective way to improve the performance of the battery is to make the cathode fulfill the following requirements.

- The material must contain a readily reducible/oxidizable ion.
- The material must react with lithium very rapidly on both lithium insertion and removal to give high power.
- The material must be low cost and environmentally friendly.
- The material should be a good electronic conductor.

Table 2.1: Specific energy (energy density) of commercialized cathode materials [21–23].

Cathode	Specific Energy (Wh/kg)
$Li(NiCoAl)O_2$ (NCA)	230
$Li(Co_xNi_yMn_z)O_2$ (NMC)	200
$LiCoO_2$ (LCO)	180
$LiMn_2O_4$ (LMO)	120
$LiFePO_4$ (LFP)	110
Li_2TiO_3 (LTO)	65

The two cathode materials that this study focused on are LCO (typically used in portable electronics) and NMC (used in electrical vehicles).

2.1.2.1 Lithium Cobalt Oxide ($LiCoO_2$)(LCO)

LCO was the first cathode that was introduced since 1980 by Oxford University and Tokyo University's Koichi Mizushima and commercialized by Sony Corporation in 1991 [24]. There are two types of LCO which are low temperature (LT-LCO) representing in cubic form and high temperature (HT-LCO) representing in hexagonal form as shown in Figure 2.2. The structure can also be described as transition metal oxide layers separated by layers of Li^+ ions, represented by green dots in Figure 2.2. The crystallinity of structure is the important feature in achieving high-performance rechargeable batteries, that is as high specific capacity, low self-discharge, and excellent cycle life as possible [25–27]. The important role of cobalt is to stabilize the cathode structure but it is costly and less available compared to other transition metals like nickel and manganese. Therefore, the further development of the cathode will focus on cheaper material such as using nickel and manganese instead of cobalt in order to reduce the cost and also environmental impact.

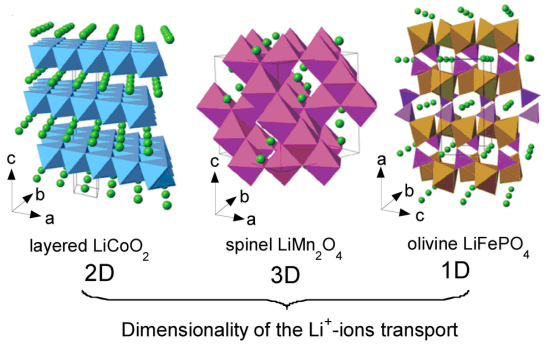

Figure 2.2: Crystal structure of the three lithium-insertion compounds in which the Li^+ ions are mobile through the 2-D (layered), 3-D (spinel) and 1-D (olivine) frameworks [28].

2.1.2.2 Lithium Nickel Manganese Cobalt Oxides ($Li(Co_xNi_yMn_z)O_2$)(NMC)

NMC is the nickel rich cathode where x+y+z is equal to 1. There are many possible ratios of cobalt, nickel and manganese such as $LiNi_{1/3}Mn_{1/3}Co_{1/3}O_2$ (NMC111), $LiNi_{0.6}Mn_{0.2}Co_{0.2}O_2$ (NMC622), and $LiNi_{0.8}Mn_{0.1}Co_{0.1}O_2$ (NMC811). According to Table 2.2, the capacity has been improved by the increase of nickel content. The capacity of NMC811 is increased by almost 31% compared to NMC111. The mixtures of cobalt, nickel, and manganese are designed to combine the specialty properties of each material together with minimizing the drawbacks. A nickel rich composition can improve the energy density of lithium-ion batteries significantly [29]. Moreover, as stated in Ozhuku et al. [30], manganese can improve thermal stability, also the addition of some aluminum such as in the NCA cathode material is expected to exhibit more thermal stability and longer cycling life.

Table 2.2: Material energy density (mAh/g) of LCO and different NMC cathode materials [31].

Cathode material	Capacity (mAh/g)
LCO	199.3
NMC111	154.8
NMC622	175.8
NMC811	203.4

2.1.3 Current collector and separator

The current collectors allow electrons to transport to (or from) the electrodes and they are located on the external surface of the electrodes. During the discharge process, it will collect charges that are generated during charging and the current collectors will permit the connection to an external circuit source [32]. The important role of current collectors is to enhance electron transfer. The current collectors are usually made from inexpensive metals and mostly in the form of a thin foil to improve the adhesive property. Materials used for positive and negative current

collector will be different due to corrosive property. For that reason, copper foil is used for the anode and aluminum foil for the cathode.

The separator is one of the important components of a LiB cell that is not involved in the electrochemical reactions (i.e., it is an isolator with no electrical conductivity). The main function is to physically separate positive and negative electrodes from each other while still allow the transport of ions [33]. Moreover, the separator prevents electrical short circuit in the cell [34]. In theory, the separator should have zero ionic resistance, but in practical, low ionic resistance is acceptable [35]. Separator can be classified into three types; porous membrane, composite separator, and non-woven mat. Nowadays, the most common separator for non-aqueous electrolytes is a porous membrane made of polyethylene (PE) and/or polypropylene (PP) [36].

2.1.4 Electrolyte

The electrolyte is one important key that determines the function of a battery. The electrolyte is a medium that allows the transport of ions in order to convert chemical energy to electrical energy, that is a high ionic conductivity is important [37]. The electrolyte is usually a lithium containing material in order to facilitate the transfer of lithium ions. The typical non-aqueous electrolyte for commercial batteries is a solution of $LiPF_6$ salt in ethylene carbonate solvent together with additives with no more than 5% of the composition [38–40]. The electrolyte additives can improve the performance by providing higher conductivity. Moreover, the electrolyte can influence the recycling process since it spreads throughout the pores of electrodes and separators. Therefore, the types of electrolyte is crucial since the electrolyte is very sensitive to other components such as electrodes. During the battery operation, a solid electrolyte interphase (SEI) will be formed on the graphite surface that compete with the reversible lithium intercalation and this determines the long-term performance of LiBs such as safety, power capability, shelf life, and cycle life [41, 42]. SEI is formed due to electrolyte decomposition after the first cycle [43]. The formation of SEI consumes electrolytes and also reduces the battery capacity. The formed SEI should prevent electrolyte decomposition and should act as a good ionic conductor to help facilitate the transport of lithium ions. Therefore, the electrolyte must be designed to contain at least one material that reacts with lithium under the formation of an insoluble electrolyte interphase.

2.2 Processes for recycling Li-ion batteries

Generally, there are four methods to recycle spent Li-ion batteries (LiBs): mechanical treatment, hydrometallurgical treatment, a combination of thermal pretreatment and hydrometallurgical treatment, or pyrometallurgical treatment. In the pyrometallurgical process, a high temperatures (above 900°C) is used and organic compounds and graphite are burned, but the process can handle a large volume of waste without any requirement of mechanical pretreatment. However, the disadvantage is that the metals cannot be fully recovered, some of them are usually left in the slag. To recover these metals, an additional hydrometallurgical process is needed. On

the other hand, hydrometallurgical processes are able to recover valuable metals at high purity and high recycle rate and the hydrometallurgical process is more environmentally friendly than the pyrometallurgical processes due to applying lower temperatures, low energy demand, and less emission of hazardous gases. Due to its great performances, hydrometallurgical processes are therefore of interest when developing recycling schemes for spent LiBs and this study will focus on dissolution of LCO and NMC cathode materials in the presence of the reducing agent hydrogen peroxide.

2.2.1 Hydrometallurgical process

Hydrometallurgical processes are used to recover valuable metals, such as cobalt and lithium, from spent LiBs. There are some pretreatment methods before a hydrometallurgical separation processes can be applied and these are mechanical and thermal pretreatments. Thermal pretreatment is also implemented in order to remove organic compounds such as binders which can cause problems in further separation steps. The process that combines both thermal pretreatment and hydrometallurgical processing is known as the combined process. It starts with discharging the spent batteries, followed by dismantling, mechanical pretreatment, thermal pretreatment, and separation stages followed by the hydrometallurgical process. Hydrometallurgical separation processes are for example leaching, solvent extraction, precipitation, ion exchange, etc. A general flowsheet of the combined process is shown in Figure 2.3. However, difference recycling schemes can be seen at different companies.

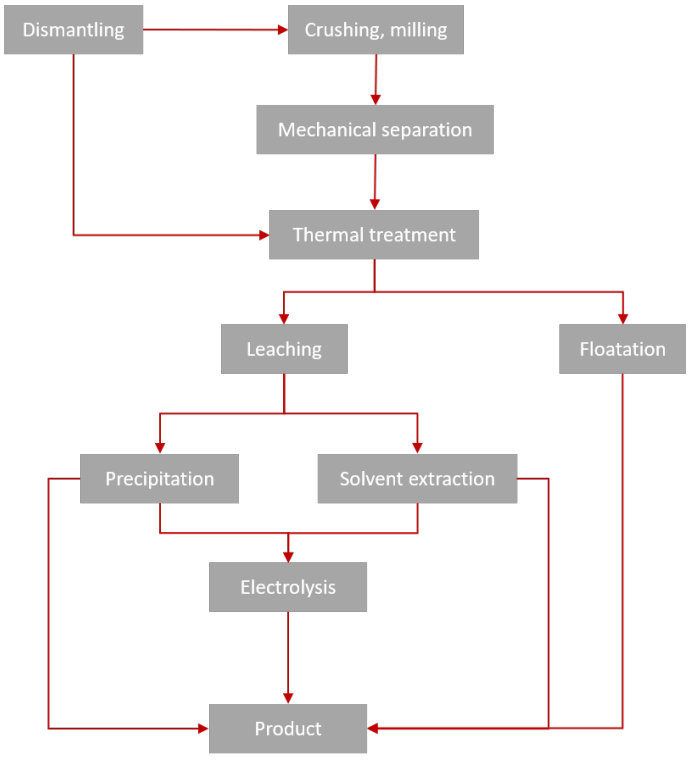

Figure 2.3: A general flowsheet for the combined recycling process [44].

2.2.1.1 Pretreatment steps

As mentioned above, the composition of LiBs is very complex and LiBs cannot be recycled directly. Therefore, several pretreatments are necessary to separate all particular components and proper management for each component can possibly be applied. The pretreatments consist of discharging, dismantling, mechanical, and thermal treatments.

Discharging

The aim of discharge is to discard the remaining capacity (remove the stored energy) in spent LiBs in order to prevent short-circuits and self-ignition. There are different discharging methods. The most common is to immerse spent LiBs in a 5 wt% NaCl solution to let them completely discharged [45, 46].

Dismantling and mechanical pretreatment

These processes are essential for large batteries such as car batteries. Dismantling is performed after discharging by removing battery cells and other components. Other components, which are cables, printed circuit boards, and casing, will be sent to recycling facilities for reprocessing in a proper way. Manual dismantling can be applied to large battery size and required several tools such as pincers, knives, and saws. Manual dismantling is not feasible for small LiBs where a mechanical pretreatment could be applied instead [47]. Methods of mechanical pretreatment involve crushing, sieving, magnetic separation, and classification which is to obtain a fraction enriched in the cathode active material (black mass). After crushing and sieving, the separator, aluminum foils, copper foils, and plastics are mainly in the coarse particles while the electrode materials, for instance LCO, and graphite, end up in fine fraction [48]. Magnetic separation is used to separate steel out based on their different magnetic properties.

At the same time, the black mass will be sent to battery recycling facilities in order to separate cathode materials from current collectors (Cu/Al foils) by dissolving the organic binders which are between them. The organic binders are made of polyvinylidene difluoride (PVDF) and organic solvents such as N,N-dimethylformamide (DMF), N,N-dimethylacetamide (DMAC), N-methylpyrrolidone (NMP), and dimethylsulfoxide (DMSO) that are used to dissolve PVDF [44] because they are all polar and can easily dissolve together. However, the dissolution process by organic solvents cannot remove all impurities. The process is also costly because of expensive solvents and not suitable for large scale. A calcination process which is a thermal process may be needed to remove (decompose) residues.

Thermal pretreatment

Additionally, thermal pretreatment is another method that could also be performed to remove organic compounds (e.g., PVDF). It is done by burning organic compounds at high temperature (typically in the range of 500-1150°C) in a furnace [49]. This process is simple and suitable for a high loaded sample but it emits toxic gases and smoke during the process which are needed to be controlled.

2.2.1.2 Leaching

After the black mass is obtained from the previous pretreatment steps, hydrometallurgical processes can be applied. The leaching process is the first step in hydromet-

allurgical processing. It is a process that extracts a certain soluble material from a solid by using solvent [50], in this case, the valuable metals presented in the black mass will be recovered as metal ions in the leachate. There are different types of leaching processes proposed for battery recycling, for example, leaching with inorganic acids, organic acids, bioleaching, and so on. In this work, the leaching using inorganic acids will be explored. The most common inorganic acids used are sulfuric acid (H_2SO_4), hydrochloric acid (HCl) and nitric acid (HNO_3). HCl gives higher leaching efficiency over the others [51, 52]. Nevertheless, once HCl is used, Cl_2 gas will be produced as can be seen in Equation 2.2 (example LCO).

$$2LiCoO_2 + 8HCl \rightleftharpoons 2CoCl_2 + Cl_2 + 2LiCl + 4H_2O \tag{2.2}$$

Chlorine gas poses an environmental problem and requires high corrosion resistance equipment which leads to higher recycling costs. The use of H_2SO_4 as an inorganic acid will be studied in this work. In addition, the leaching efficiency has also been shown to increase with the use of a reducing agent like hydrogen peroxide (H_2O_2). The main purpose with addition of a reducing agent is to change the valence state of the metals used in the cathode active material into a more soluble state (e.g. Co^{3+} to Co^{2+}) and by that increases the leaching efficiency. Oxygen is generated as a consequence of the reaction between hydrogen peroxide and the black mass. In the presence of H_2O_2 in H_2SO_4 leaching, the cobalt leaching efficiency can be increased by 13% [53]. Incorporation of H_2SO_4 and H_2O_2 yields leaching efficiency of valuable metals as high as when using HCl [54, 55]. Table 2.3 summarizes the related literature about leaching processes, optimum leaching conditions, and metal recovery yields.

Table 2.3: Summary of related literature about leaching process.

Leaching media	S:L (g/L)	Temperature (°C)	Leaching time (hr)	Co leaching efficiency (%)	Li leaching efficiency (%)	Reference
2M H_2SO_4, 5vol% H_2O_2	50	80	1	99	99	[54]
4M HCl	20	80	1	99.5	99.9	[55]
1M H_2SO_4	50	95	4	66.2	93.4	[53]
1M H_2SO_4, 5vol% H_2O_2	50	95	4	79.2	94	[53]

The proposed sulfuric acid leaching reactions for the different cathode materials studied, without any reducing agent present, are shown as Equations 2.3, 2.4, 2.5, and 2.6 which represent LCO, NMC111, NMC622 and NMC811, respectively.

$$4LiCoO_2(s) + 6H_2SO_4(aq) \rightleftharpoons 4CoSO_4(aq) + 2Li_2SO_4(aq) + 6H_2O(l) + O_2(g) \tag{2.3}$$

$$12LiNi_{0.33}Mn_{0.33}Co_{0.33}O_2(s) + 18H_2SO_4(aq) \rightleftharpoons 4NiSO_4(aq) + 4CoSO_4(aq) + 4MnSO_4 + 6Li_2SO_4(aq) + 9H_2O(l) + 3O_2(g) \tag{2.4}$$

$$20LiNi_{0.6}Mn_{0.2}Co_{0.2}O_2(s) + 30H_2SO_4(aq) \rightleftharpoons 12NiSO_4(aq) + 4CoSO_4(aq) + 4MnSO_4 + 10Li_2SO_4(aq) + 30H_2O(l) + 5O_2(g) \tag{2.5}$$

$$20LiNi_{0.8}Mn_{0.1}Co_{0.1}O_2(s) + 30H_2SO_4(aq) \rightleftharpoons 16NiSO_4(aq) + 2CoSO_4(aq) + 2MnSO_4 + 10Li_2SO_4(aq) + 30H_2O(l) + 5O_2(g) \tag{2.6}$$

Moreover, the corresponding leaching reactions using sulfuric acid as leaching agent and the addition of H_2O_2 as reducing agent are shown below.

$$2LiCoO_2 + 3H_2SO_4 + H_2O_2 \rightleftharpoons 2CoSO_4 + Li_2SO_4 + 4H_2O + O_2 \tag{2.7}$$

$$6LiNi_{0.33}Mn_{0.33}Co_{0.33}O_2(s) + 9H_2SO_4(aq) + H_2O_2 \rightleftharpoons 2NiSO_4(aq) + 2CoSO_4(aq) + 2MnSO_4 + 3Li_2SO_4(aq) + 10H_2O(l) + 2O_2(g) \tag{2.8}$$

$$10LiNi_{0.6}Mn_{0.2}Co_{0.2}O_2(s) + 15H_2SO_4(aq) + H_2O_2 \rightleftharpoons 6NiSO_4(aq) + 2CoSO_4(aq) + 2MnSO_4 + 5Li_2SO_4(aq) + 16H_2O(l) + 3O_2(g) \tag{2.9}$$

$$40LiNi_{0.8}Mn_{0.1}Co_{0.1}O_2(s) + 60H_2SO_4(aq) + 2H_2O_2 \rightleftharpoons 32NiSO_4(aq) + 4CoSO_4(aq) + 4MnSO_4 + 20Li_2SO_4(aq) + 62H_2O(l) + 11O_2(g) \tag{2.10}$$

As mentioned before, hydrogen peroxide can be an effective reducing agent to leach valuable metals from spent batteries. Table 2.4 summarizes some literature that describes the effect of hydrogen peroxide on the leaching with hydrogen peroxide.

Table 2.4: Summary of related literature about sulfuric acid leaching process co-operated with hydrogen peroxide.

Material	Leaching condition	Optimal amount of H_2O_2	H_2O_2 adding pattern	Co leaching efficiency (%)	Li leaching efficiency (%)	Reference
Spent LiBs	4 M H_2SO_4, S:L=1:10, T=85°C	10 vol%	Initial adding	95	96	[56]
Spent LiBs	2 M H_2SO_4, S:L=1:20, T=75°C	10 vol%	Initial adding	80	99	[57]
Spent LiBs	2 M H_2SO_4, S:L=1:10, T=75°C	5 vol%	Initial adding	70	99.1	[58]

As a whole, most of the literature describes the sulfuric acid leaching with addition of H_2O_2 as a reducing agent where the proposed amount of H_2O_2 was added at the beginning of the leaching process. However, no one has studied the remaining amount of hydrogen peroxide that might be still left after leaching and different hydrogen peroxide adding strategies. The novelty of this study is to investigate the residual amount of hydrogen peroxide as well as assess different hydrogen peroxide addition strategies.

2.2.1.3 Solvent extraction and precipitation

After the metals such as Li, Co, Ni, Mn, Cu, Al, Fe are leached from the cathode active material, they still need to be recovered from the leachate. Other hydrometallurgical methods, such as solvent extraction, precipitation, and electrochemical deposition, are needed in order to separate and recover these metals. Compared to precipitation, solvent extraction has a better separation effect due to its selectivity of extractants. Since the leaching solution is complex, more than one technique could be used to separate pure metals effectively [59].

Solvent extraction

Basically, the process consists of two immiscible liquid phases: organic and aqueous phases. It involves two operations: Extraction and stripping. Extraction refers to when the metals in the aqueous phase are transferred to the organic phase where the metals are more soluble into. Extraction is followed by stripping where the extracted metals are recovered from the organic phase to another strip solution [50].

There are several extractants that could be used depending on the selectivity of the desired metal and operating pH. Examples of extractants are di-(2-ethylhexyl) phosphoric acid (D2EHPA), diethylhexyl phosphoric acid (DEHPA), bis-(2,4,4-tri-methyl-pentyl) phosphinic acid (Cyanex 272), trioctylamine (TOA), and 2-ethylhexyl phosphonic acid mono-2-ethylhexyl ester (PC-88A) [47]. Figure 2.4 summarizes suitable extractants and the operating pH to extract a specific metal ion. Some of the extractants can recover more than one metal ion by using several

stages in a series with different extractants. According to [60], D2EHPA was good at extracting copper and manganese ions at a pH range of 2.6-2.7 and PC-88A was then used to recover cobalt and nickel ions at pH 4.5.

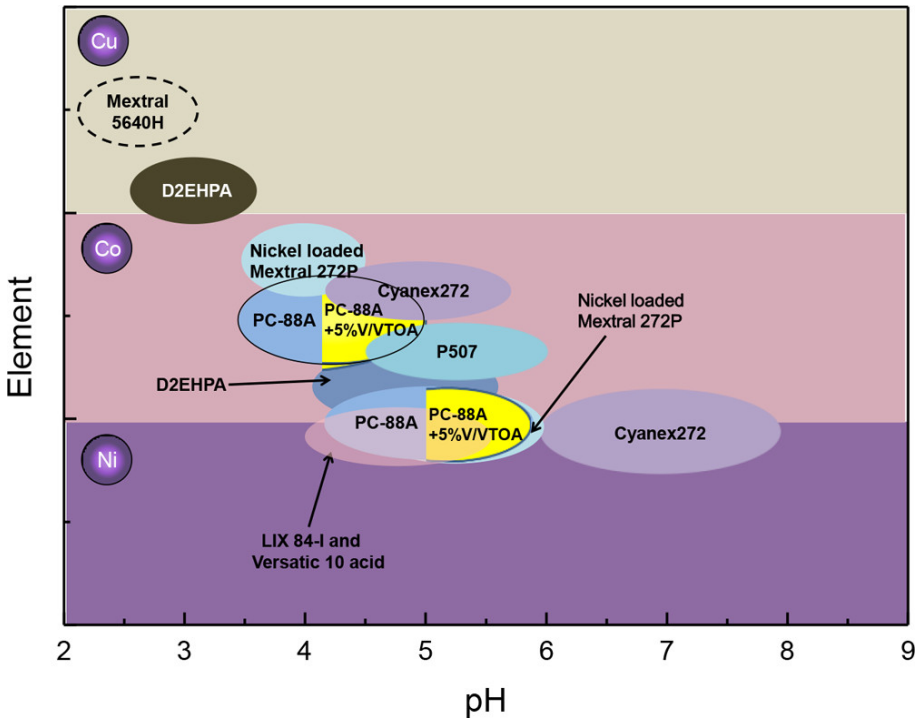

Figure 2.4: Suitable extractants for extracting nickel, cobalt, and copper at different pHs [60–65].

Precipitation

Precipitation is an alternative to recover metals. Precipitants containing anions such as OH^-, $C_2O_4{}^{2-}$ and $CO_3{}^{2-}$ are added into a leaching solution and then anions will attract to metal cations and form insoluble precipitates which can easily be extracted out. Sometimes, one metal ion is hard to be precipitated when other metal also has the same valence state, such as Co^{2+} and Ni^{2+}, and the coprecipitation of both metals can occur. As a result, [51] showed that Co^{2+} in the leaching liquor was oxidized to Co^{3+} by adding sodium hypochlorite (NaClO) to recover $Co_2O_3 \cdot 3H_2O$ by selective precipitation and nickel hydroxide is further precipitated by addition of a base. Moreover, precipitation could usually be used before solvent extraction in order to remove impurities, such as aluminum, copper, and iron, that will hinder the separation of cobalt in the solvent extraction process [44].

According to all mentioned recycling processes, the final recovered metals can possibly be reused in batteries or in other applications to move toward the circular economy promoted by restrictive environmental regulations and limited natural resources. In 2018, the recycling of spent NMC523 and LFP can be profitable based on China's background with the profits of 2256 Euro/ton and 436 Euro/ton, respectively [66]. However, today's recycling methods need to be improved to save energy, chemicals and time required as much as possible in order to be more cost-effective and more accessible.

2.3 Aim and objective

Due to a rapid increase in the demand of Li-ion batteries, stockpiles of spent batteries have been produced globally. The hydrometallurgical process is an interesting recycling method that is environmentally-friendly and effectively recovers valuable metals but it is not cost-effective. In order to make it economically feasible, the process parameters should be optimized. The aim and objective of this study is to:

- Determine the effect of adding a reducing agent, which is hydrogen peroxide, on different types of battery active materials (LCO, NMC111, NMC622, and NMC811).
- Optimize the operating parameters in the leaching process namely leaching temperature, acid concentration, solid-to-liquid ratio, and addition strategy and amount of hydrogen peroxide.
- Examine whether hydrogen peroxide can be used efficiently to recover valuable metals from industrially mechanically pre-treated spent Li-ion batteries. A deeper understanding on how H_2O_2 influence on leaching process with different surrounding conditions were examined in order to maximize the leaching efficiency along with the reduction of time, solvent and energy used.

2.4 Scope of work

Four different types of cathode material were studied: LCO, NMC111, NMC622, and NMC811. Lithium ion batteries of LCO type is common in portable electronics and NMC-type batteries in electrical vehicles. These cathode materials are now being used nowadays. This work will study the leaching process, which is a part of the hydrometallurgical process to recycle spent batteries, using sulfuric acid as a leaching agent with the help of hydrogen peroxide as a reducing agent.

3

Methods

3.1 Materials and reagents

The cathode materials used in this study are LCO and mixed NMC including NMC111, NMC622, and NMC811. LCO used was a pure metal oxides from Sigma-Aldrich which is in black powder form. Whereas the mixed NMCs were provided by Uppsala university and are also in pure form. The sulfuric acid is an essential leaching agent in the leaching process of active cathode materials of LiBs. The different concentrations of sulfuric acid were prepared from concentrated (95% - 97%) solution that was supplied by Sigma-Aldrich. The Hydrogen peroxide that was used as a reducing agent was kindly supported from Nouryon Functional Chemicals AB, the solution has 59-59.5 wt.% (EKA HP C59). Moreover, the aluminum foil and copper metal powder were used as current collectors that can present in spent Li-ion batteries. The real NMC cathode waste material was provided by Volvo Cars and mechanically treated at Akkuser in Finland. The material was dissolved in aqua regia for 5 hours at 80°C and then analyzed by ICP-OES.

3.2 Leaching

The leaching processes were done by using sulphuric acid as leaching reagent. The desired concentration of sulphuric acid was prepared by diluting high concentrated sulphuric acid with Milli-Q water. The process was carried out in either 100 mL plastic beaker or 20 mL glass bottle depending on the desired amount of liquid and it was immersed in the glass water bath for temperature control. The container was covered with the lid to reduce the loss of water from evaporation. It was agitated by a magnetic stirrer at 300 rpm in order to improve mixing efficiency, and regulated to the desired temperature before introducing cathode material powder. The leaching time was started recording after the black mass powder was added. All experiments were done in triplicates. The sampling times were at 1, 5, 10, 15, 30, and 60-minute when only sulfuric acid was added. When hydrogen peroxide was added, the sampling times were changed to 1, 2, 3, 15, 30, and 60-minute. Each sampling time, more than 200 μL of leaching sample was withdrawn from the beaker to get enough volume for the analysis and immediately filtered by a syringe filter with pore size of 0.45 μm and 25mm in diameter. Only 100 μL of leaching sample was actually taken out and the rest of the solution and 100 μL of sulfuric acid will be returned to the leaching solution to minimize the change of solid-to-liquid ratio. The obtained 100 μL samples were first diluted by addition of 9.9 mL of 0.5 M nitric acid. The

second dilution is necessary before the ICP-OES analysis. The sample was diluted as a factor of 1000. Each 1 mL of diluted sample was diluted again with 9 mL of 0.5 M nitric acid.

3.3 Determination of metal concentration in leaching solution

Metal concentrations in each leaching solution were determined by using ICP-OES. The calibration curve was prepared by using the metal solution with the concentration of 0 ppm, 5 ppm, 10 ppm and 20 ppm. The new set of standard solutions was prepared every time when using ICP-OES measurement since the variation of concentration can be occurred due to temperature change. Firstly, standard solution of 20 ppm was prepared by using 1000 ppm metal concentration that is provided by SPEX CertiPrep (SPEX CertiPrep Group, Metuchen, US). In this case, there are 4 main metals that are focused on so each 1 mL of lithium, cobalt, manganese and nickel is diluted with 0.5 M nitric acid until the volume reaches 50 mL in order to make 20 ppm. Then 10 ppm and 5 ppm standard solution were prepared by dilution from 20 ppm.

The suitable wavelength was selected for each metals that needed to analyze. The multiple wavelength can be selected however it should exhibit suitable intensities and also free from spectral interferences. In this experiment the following wavelengths that show in Table 3.1 were used for the analysis:

Table 3.1: Selected wavelengths in ICP-OES analysis

Metal element	Selected Wavelength (nm)
Li	670.784
Co	228.616
Ni	221.648
Mn	257.61
Al	396.153
Cu	327.393

To calculate leaching efficiency, the equation 3.1 and 3.2 are used.

$$\text{Leaching efficiency } [\%] = \left[\frac{(C/1000) \cdot V}{m_{metal}}\right] \cdot 100 \tag{3.1}$$

C is specific metal concentration obtained from ICP-OES analysis [ppm].

V is the volume of leaching solution [mL].

m_{metal} is the amount of certain metal in the cathode material used [g] which is calculated from Equation 3.2.

$$m_{metal} = \left(\frac{MW_{metal} \cdot \text{Molar ratio}}{MW_{cathode}}\right) \cdot m_{cathode} \tag{3.2}$$

MW_{metal} is the molecular weight of specific metal [g/mol].

Molar ratio is the molar ratio of specific metal in cathode material chemical formula, for example, the molar ratio of Co is 0.33 in $LiNi_{0.33}Mn_{0.33}Co_{0.33}O_2$ (NMC111) [-].

$MW_{cathode}$ is the molecular weight of specific cathode material [g/mol].

$m_{cathode}$ is the weight of cathode material [g].

3.4 Determination of hydrogen peroxide in leaching solution

The hydrogen peroxide that was used in all experiments was provided by Nouryon under brand name Eka HP C59 which has H_2O_2 content around 59 - 59.5 wt.%. The residual concentration in solution was determined using iodometric method. All chemicals used in this method are listed as followings:

- 2 M Sulfuric acid (H_2SO_4)
- 1 M Potassium Iodide solution (KI)
- Ammonium molybdate ($(NH_4)_6Mo_7O_{24}{\cdot}4H_2O$) 15% solution
- 0.05 M Sodium thiosulfate solution ($Na_2S_2O_3$)
- Iodine indicator

For the determination, the sample should be filtered first. For 1-10 vol% H_2O_2, a sample volume of 200 μL is suitable for the titration. The sample should be adjusted with deionized water to a volume of 50 mL then followed by the addition of 5 mL sulfuric acid and 10 mL of potassium iodide. A few drops of ammonium molybdate were added and the titration was done immediately with sodium thiosulfate solution to a light-yellow color. A few drops of iodine indicator were added and continue to titrate until the solution was colorless. To prevent the decomposition of hydrogen peroxide, the titration was performed immediately after each sampling time. The results were not corrected for interfering substances present in the leaching solution and a minor discrepancy may therefore occur.

The following equation was used to calculate the remaining concentration of hydrogen peroxide.

$$\text{Residual hydrogen peroxide [g/L]} = \left[\frac{V_{Na_2S_2O_3} \cdot C_{Na_2S_2O_3} \cdot MW}{n \cdot V_{prov}}\right] \tag{3.3}$$

$V_{Na2S2O3}$ is the volume of sodium thiosulfate solution used in titration (mL).

MW is the molecular weight for hydrogen peroxide which is 34 g/mol.

n is the equimolar factor which is 2.

V_{prov} is the volume of sample (mL)

4

Results

4.1 Effect of leaching temperature

The leaching process was performed at two different temperatures which are 50°C and 60°C in order to determine the most suitable temperature in terms of performance, energy demand and economics. The overall leaching time was 60 minutes. The solid-to-liquid ratio of 1:100 g/mL was fixed and 50 mL of sulfuric acid was used. Each experiment was done in triplicates. In every figures, the y-axis represents the metal leaching efficiency and the x-axis represents leaching time from 0 to 60 minutes. Standard deviation was also calculated and presented in all figures as vertical error bars.

4.1.1 Leaching of LCO

Figures 4.1a and 4.1b represent the leaching efficiencies of lithium and cobalt respectively for LCO. All points show the average value from three replicates. Only lithium and cobalt leaching were in focus for this cathode material.

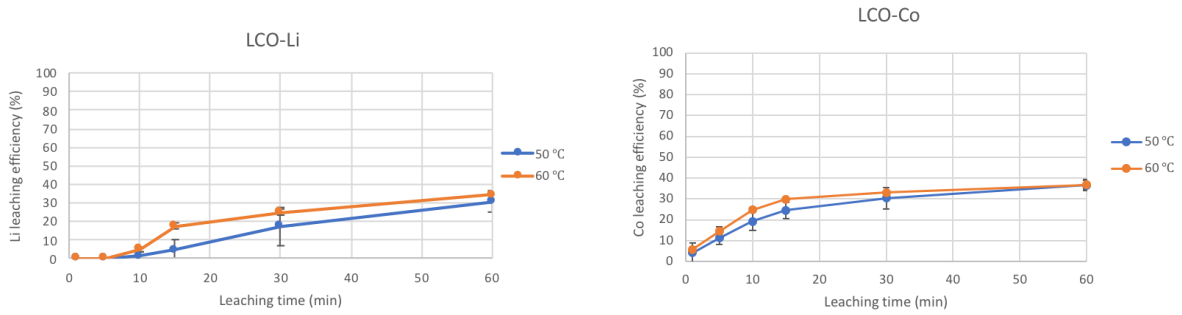

(a) Li leaching efficiency **(b)** Co leaching efficiency

Figure 4.1: Leaching of LCO: Influence of temperature (reaction conditions: 2 M H_2SO_4, no H_2O_2, solid-to-liquid ratio of 1:100 (50 mL solution)).

For lithium leaching in Figure 4.1a, both temperatures illustrated the same trend. In the first 5 minutes of leaching time, nothing was dissolved. There was no lithium represented in the leaching solution so that the leaching efficiency become zero for both temperatures. Leaching efficiency started to increase after 10 minutes. The highest standard deviation was observed at 30 minutes. At 60 minutes,

the highest efficiency was obtained for both 50°C and 60°C; the highest leaching efficiency was 34.5% at 60°C which is only 4% higher than at 50°C.

In Figure 4.1b, the leaching of cobalt is represented. The leaching efficiency of cobalt in LCO was slightly higher compared to lithium leaching. The leaching performance increased from the beginning and increased only a few percentages after 30 minutes. For both temperatures, the highest leaching efficiency was obtained after 60 minutes and was around 36%. There was no significant difference between the two temperatures, i.e. 50°C was preferable.

4.1.2 Leaching of NMC111

In this section, Figures 4.2a, 4.2b, 4.2c, and 4.2d show the kinetic leaching curve of Li, Co, Ni, and Mn which are the main four elements in the mixed cathode material. The leaching process was operated in both 50°C and 60°C to find the optimal temperature.

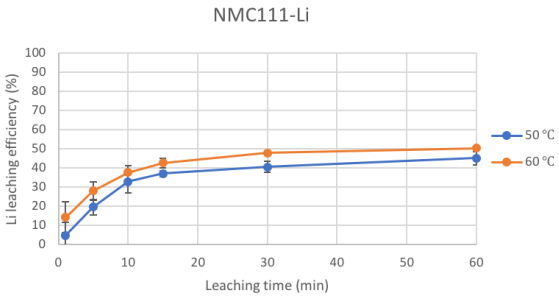

(a) Li leaching efficiency

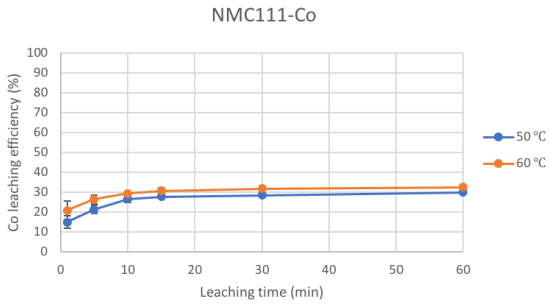

(b) Co leaching efficiency

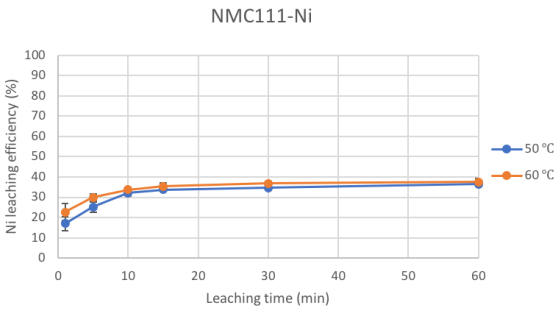

(c) Ni leaching efficiency

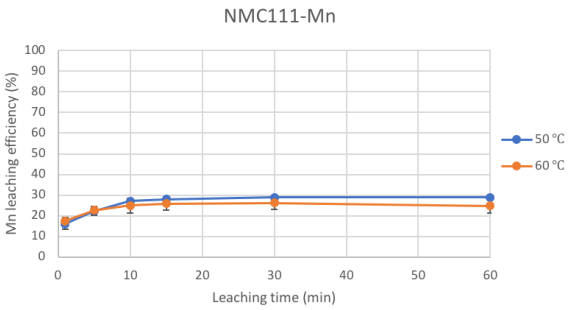

(d) Mn leaching efficiency

Figure 4.2: Leaching of NMC111: Influence of temperature (reaction conditions: 2 M H_2SO_4, no H_2O_2, solid-to-liquid ratio of 1:100 (50 mL solution)).

In Figure 4.2a, the leaching efficiency of lithium increased considerably and increased gently after 15 minutes for both temperatures. The leaching process at 60°C showed slightly higher performance during the overall leaching time. The highest leaching efficiency was reached after 60 minutes for both temperatures. The maximum leaching efficiency was at 60°C and was 50.3%.

In Figure 4.2b, cobalt leaching is illustrated. The leaching efficiency increased slowly and leveled off after 15 minutes. Both temperatures showed almost identical performance but all values at 60°C always showed superior result. During the last 30 minutes of leaching process at 60°C equilibrium was reached, and the efficiency increased less than 1%. The maximum leaching efficiency was 32.4%.

In Figure 4.2c, the nickel leaching performance at 60°C was slightly higher than at 50°C during the first 5 minutes of leaching. After that, the leaching efficiency was about the same for both temperatures and was about 37% at 60 minutes.

In the case of Mn in Figure 4.2d, the trend of kinetic curves were almost identical for both temperatures. Both leaching efficiency increased slowly during the first 15 minutes. After 15 minutes, the leaching performance was almost stable. The maximum efficiency was obtained at 50°C/60 minutes and was about 28.8%; a better performance compare with 60°C. Therefore, the more suitable temperature was 50°C since the performance at 60°C was not significantly better.

4.1.3 Leaching of NMC622

The figures in this section show the leaching efficiency for NMC622. Four valuable metals including Li, Co, Ni and Mn, which are the main component in this mixed NMC cathode material, are also of an interest and measured in concentration for calculating the leaching efficiency and comparing the results.

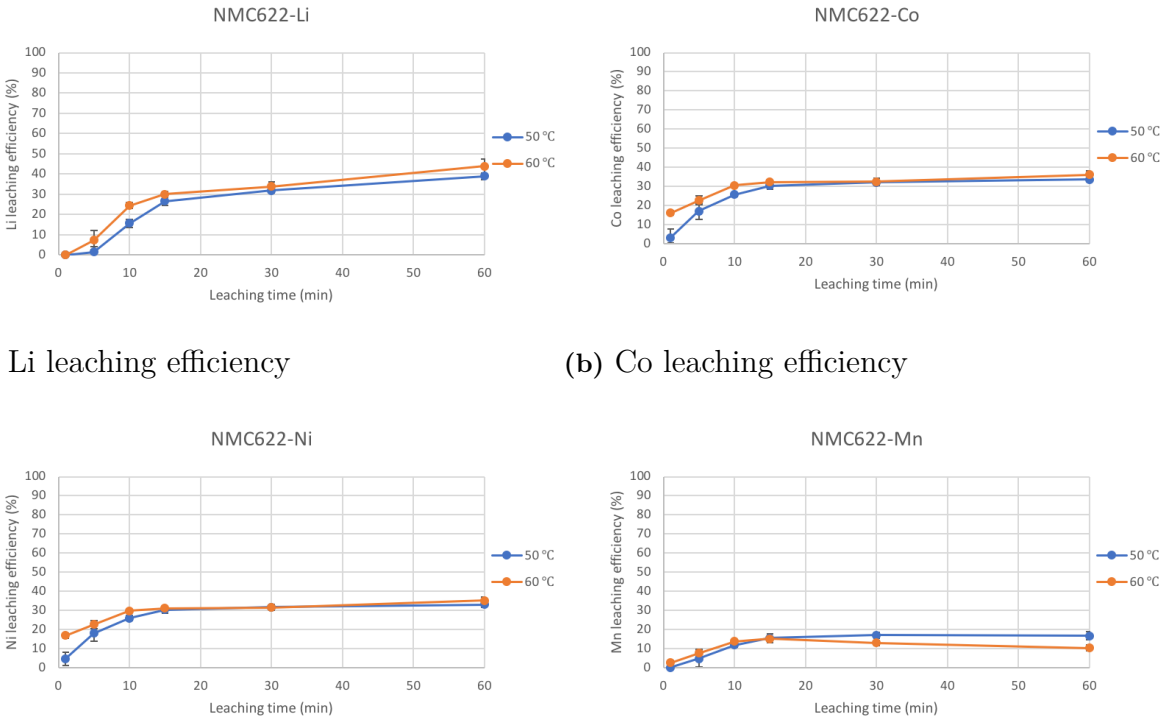

(a) Li leaching efficiency

(b) Co leaching efficiency

(c) Ni leaching efficiency

(d) Mn leaching efficiency

Figure 4.3: Leaching of NMC622: Influence of temperature (reaction conditions: 2 M H_2SO_4, no H_2O_2, solid-to-liquid ratio of 1:100 (50 mL solution)).

Figure 4.3a represents the leaching efficiency of lithium from NMC622. The curve clearly showed that the lithium leaching efficiency increased when time passed for both temperatures. At 60°C, the leaching efficiencies are slightly higher than operating at 50°C for all sampling points. The reason behind this is that an increase in temperature can accelerate molecules to move faster and increase energy of particles [67]. The maximum Li leaching efficiencies after 60 minutes leaching time were approximately 39% and 44% for 50°C and 60°C, respectively.

Figure 4.3b represents the leaching kinetic of cobalt from NMC622. The trend of the curves was the same as for lithium (Figure 4.3a). Leaching at 60°C yields marginally higher cobalt leaching efficiency than at 50°C for all plots and shows better leaching performance as seen as higher efficiency (almost 20%) was reached at the beginning. After 15 minutes, the curves tended to reach constant efficiencies. The maximum cobalt leaching efficiencies of 34% and 36% obtained after 60 minutes leaching at 50°C and 60°C, respectively.

Figure 4.3c shows the leaching curve of nickel from NMC622. The nickel leaching efficiency increases in the first 10–15 minutes. A small increase in efficiency in the first 15 minutes was obtained when 60°C was used. After that, about the same values of efficiency were measured for both temperatures. After 30 minutes, the curves for both 50°C and 60°C also reached the equilibrium and approached about 33% and 35% efficiency, respectively.

Figure 4.3d represents the graph plotted between manganese leaching efficiency and time for the leaching of NMC622. At 50°C, the efficiency slightly increased in the first 30 minutes and remained constant afterward reaching a leaching efficiency of about 16.6%. The kinetic curve for 60°C went up and reached its peak after 15 minutes. Then the curve went down gradually and stayed below that of 50°C. To conclude, for leaching of manganese, 50°C tended to be more effective than 60°C.

Therefore, it was shown that there was no significant improvement on efficiency when a higher temperature was used. 50°C could be considered to be the optimal temperature to leach NMC622 in order to avoid an unnecessary high energy demand.

4.1.4 Leaching of NMC811

The figures shown in this section present the graphs plotted between leaching efficiency of a specified metal and leaching time for the leaching of mixed NMC811. Two temperatures which are 50°C and 60°C were studied.

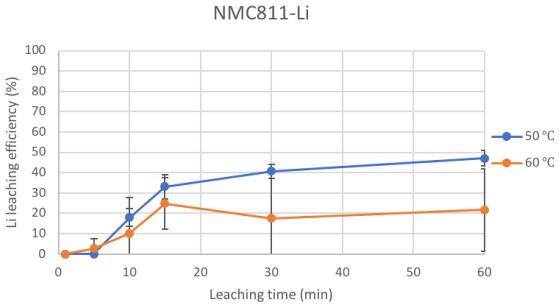

(a) Li leaching efficiency

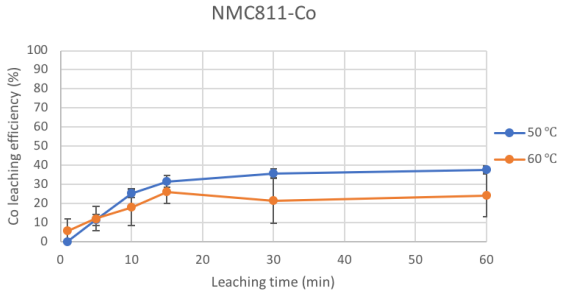

(b) Co leaching efficiency

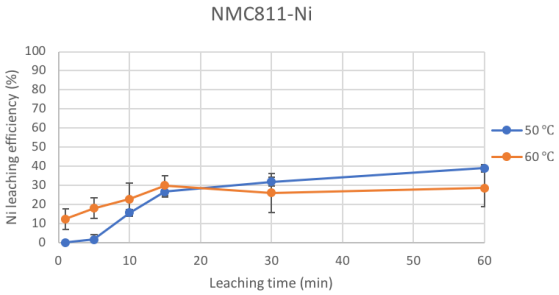

(c) Ni leaching efficiency

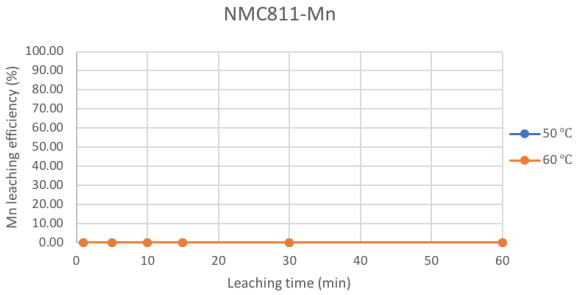

(d) Mn leaching efficiency

Figure 4.4: Leaching of NMC811: Influence of temperature (reaction conditions: 2 M H_2SO_4, no H_2O_2, solid-to-liquid ratio of 1:100 (50 mL solution)).

Figure 4.4a shows the leaching curve for lithium from NMC811. At the beginning, the efficiencies measured were rather low. The reason behind this may be because the NMC811 was hydrophobic that made it hard to be dissolved when initially added into the leaching solution. Beyond this point, the efficiency continuously increased when 50°C was used. On the other hand, for 60°C, the curve was getting higher to its peak after 15 minutes leaching and dropped down after that. The highest lithium leaching efficiencies that could be reached were 47% and 25% for 50°C and 60°C, respectively. Therefore, 50°C yielded better lithium leaching performance for NMC811.

Figure 4.4b displays the curves plotted between cobalt leaching efficiency and leaching time. It can be seen that at 50°C the efficiency increased significantly in the first 15 minutes and then increased to some extent afterwards, while at 60°C, the efficiency also increased in the first 15 minutes until it reached the maximum value and then declined to lower values. Almost 40% efficiency was reached for 50°C after 60 minutes leaching, whereas 26% for 60°C (at 15 minutes). Therefore, 50°C is more effective to leach cobalt from NMC811.

Figure 4.4c presents the nickel leaching efficiency for leaching of NMC811. As a result, the same pattern as before was observed. At 50°C, the efficiency of 40% was reached after 60 minutes leaching, when at 60°C the highest efficiency was measured as 30% after 15 minutes. Correspondingly, the lower temperature gives a better nickel leaching from NMC811.

The manganese leaching performance can be seen in Figure 4.4d. No leached manganese concentration was detected by ICP-OES regardless of leaching temperature. This was probably because of too low manganese concentration detected in the leachate.

In respect to the results, 50°C was more suitable for being used to leach valuable metals from NMC811 because such temperature yielded better leaching performance than 60°C and showed more clear pattern of leaching curves. To compare the results, a bar graph showing the leaching efficiency at the end of leaching (60 minutes) for both temperatures (50, 60°C) can be seen below. Blue bars represent 50°C and orange bars represent 60°C, vice versa.

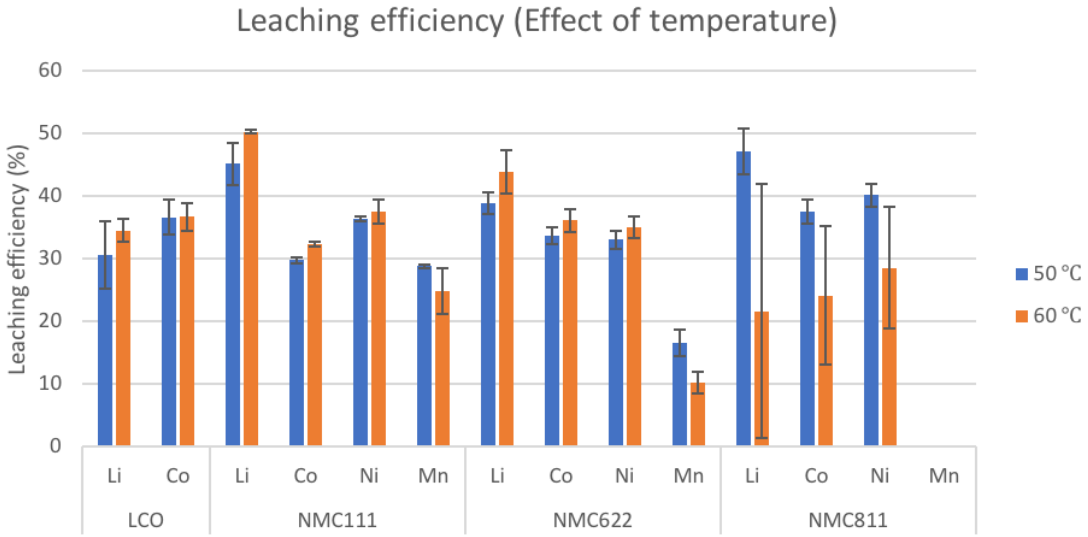

Figure 4.5: Leaching efficiency after 60 minutes leaching of all cathode materials: Influence of temperature (reaction conditions: 2 M H_2SO_4, no H_2O_2, solid-liquid ratio of 1:100 (50 mL solution)).

Based on the above results, Figure 4.5, the higher temperature (60°C) did not improve the leaching performance significantly. In some cases, especially the manganese leaching of mixed NMC cathode material, 60°C always gave a worse efficiency compared to 50°C. Moreover, the NMC811 leaching efficiency was lower when 60°C leaching temperature was used for all leached metals. Therefore, 50°C was chosen for the further experiments.

4.2 Effect of mixing

The effect of mixing was studied by using a solid-to-liquid ratio of 1:100. Two sets of experiments conducted by varying the leaching volume (10 and 50 mL). The different container was used: 20 mL smaller glass vial and 100 mL bigger and wider-in-width plastic container. An equal size of magnet was used for stirring which is more fit with small glass vial and it is expected to have a better mixing. The following figures show the leaching efficiency of all cathode materials in different leaching scales. The

thick line represents the leaching in 50 mL and thin line represents the leaching in 10 mL solution.

4.2.1 Leaching of LCO

In this section, the leaching of LCO is presented. The leaching volume was altered between 10 mL and 50 mL. The comparison of the leaching efficiency between the two different volumes is shown in Figure 4.6.

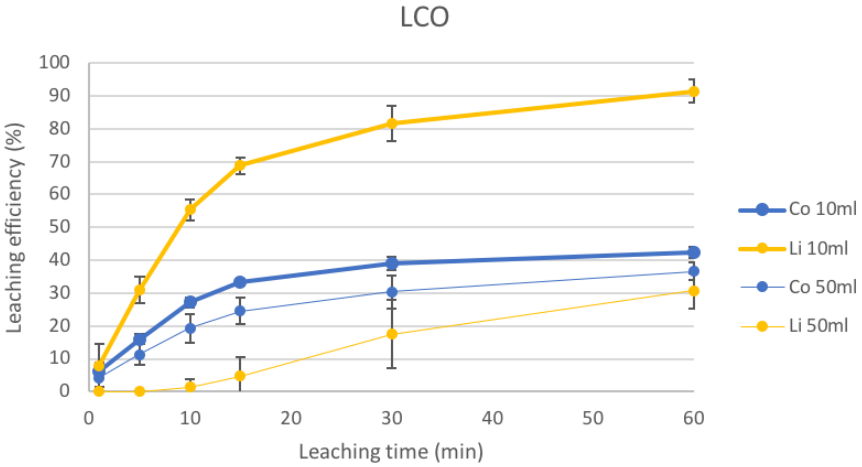

Figure 4.6: Leaching of LCO: Influence of mixing (reaction conditions: 2 M H_2SO_4, T=50°C, no H_2O_2, solid-to-liquid ratio of 1:100 (10 and 50 mL solution)).

According to Figure 4.6, the leaching process in 10 mL solution showed higher leaching performance throughout the whole leaching time. Moreover, the highest leaching efficiency that could be achieved was much higher compared to when leaching in 50 ml scale which were 91.5% and 30.7%, respectively. In addition, the cobalt leaching efficiency was also higher but not as much as when compared to lithium leaching since lithium is monovalent and can be leached more easily especially with a perfect mixing. On the other hand, cobalt leaching strongly depends on the change of oxidation state, a better mixing alone was probably not enough to overcome its limitation and a reducing agent might be needed in order to enhance leaching performance. Therefore, it was clear that decreasing the leaching volume (i.e. better mixing) can improve the leaching efficiency.

4.2.2 Leaching of NMC111

Leaching of NMC111 was performed using two different leaching containers with different volumes. The result of leaching efficiency is shown below.

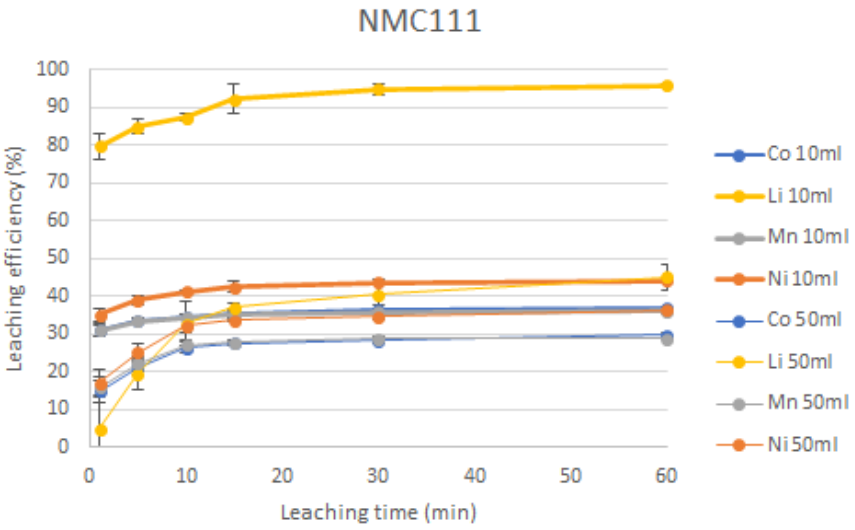

Figure 4.7: Leaching of NMC111: Influence of mixing (reaction conditions: 2 M H_2SO_4, T=50°C, no H_2O_2, solid-to-liquid ratio of 1:100 (10 and 50 mL solution)).

According to Figure 4.7, the NMC111 kinetic leaching curve showed that a higher efficiency was reached when scaling down, and the improvement was obtained already in the initial phase of leaching. It was also obvious that the lithium leaching performance was noticeably improved more than for the other metals. The lower leachability of other metals are, as for LCO, related to the need to change into the lower oxidation state while lithium is not involved with this leaching principle. The highest leaching efficiency obtained was 96% for lithium.

4.2.3 Leaching of NMC622

NMC622 leaching was focused on in this part. Figure 4.8 shows the leaching performance for the two different scales.

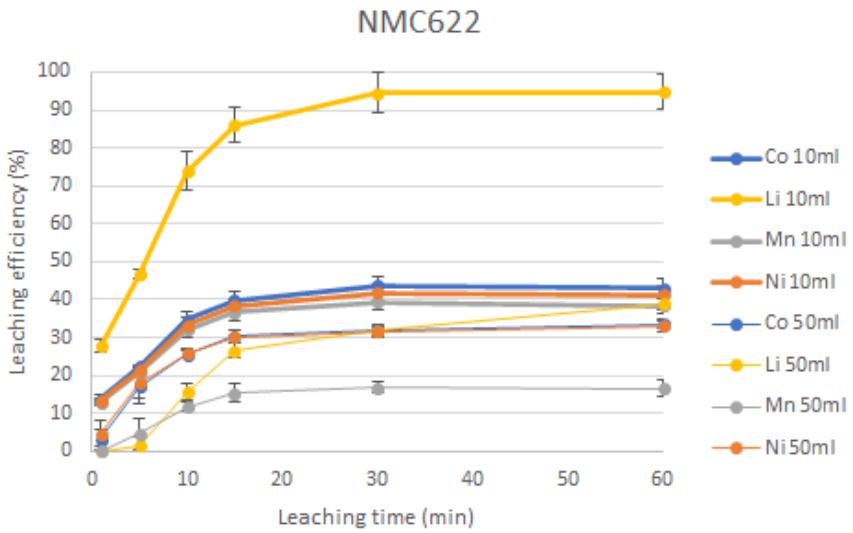

Figure 4.8: Leaching of NMC622: Influence of mixing (reaction conditions: 2 M H_2SO_4, T=50°C, no H_2O_2, solid-t0-liquid ratio of 1:100 (10 and 50 mL solution)).

From Figure 4.8, lithium was always the most easily leached element in all cathode materials. The lithium leaching almost reached 100% without any additional reducing agents while the leaching efficiency for the other elements was below 50%. A higher efficiency was achieved when the small volume was used.

4.2.4 Leaching of NMC811

NMC811 leaching was of interest since this cathode chemistry represents the latest development. The figure below reviews the influence of mixing in term of metals' leaching efficiency.

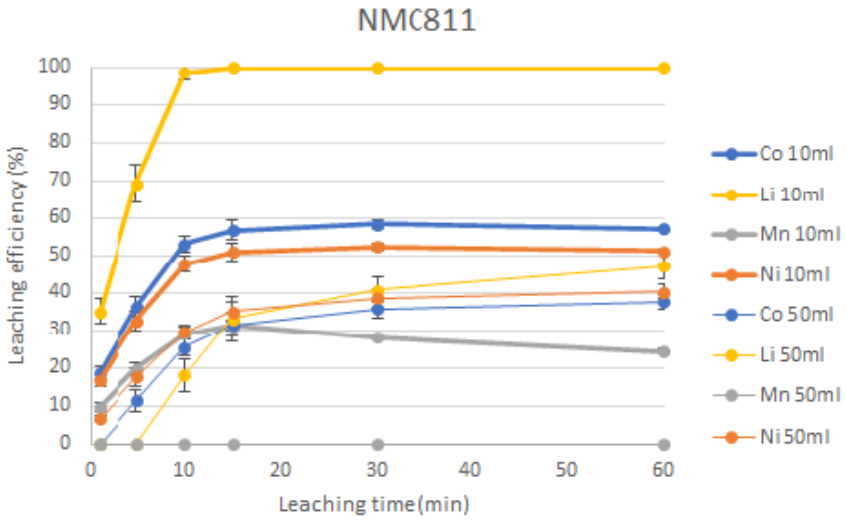

Figure 4.9: Leaching of NMC811: Influence of mixing (reaction conditions: 2 M H_2SO_4, T=50°C, no H_2O_2, solid-to-liquid ratio of 1:100 (10 and 50 mL solution)).

In the case of NMC811 that is illustrated in Figure 4.9, the lithium leaching performance reached 100% after only 15 minutes when leaching using 10 mL. Furthermore, the maximum manganese leaching efficiency was 31.2% when leaching using the smaller volume (10 mL) whereas nothing could be leached when using 50 ml. The leaching performance leveled off after 10-15 minutes for all materials and all metals.

Therefore, the leaching process should be performed using efficient mixing condition in order to maximize the leaching performance. However, the leaching was done in a less efficient mixing, 100 mL container, for the further experiments for the reason that a high volume of solution is required in order to avoid the changing the leaching volume when taking samples for analysis. The results from this section therefore cannot be compared with other experiments using different leaching volume because of the different mixing. In addition, the particle size and distribution of the cathode materials could also affect the leaching efficiency more or less. Apart from the mixing, those factors can also be interesting to study.

4.3 Effect of acid concentration

In this section, the solid-to-liquid ratio was increased in order to see whether the desired concentration of acid, which is 2 M of H_2SO_4, is sufficient. The solid-to-liquid ratio was varied as 1:100, 1:20, and 1:10 g/mL. By increasing the solid-to-liquid ratio, there will be less acid to leach the desired metals and amount of acid can be a limiting factor, i.e. a higher acid concentration might be needed. The calculations to find the limiting agent in the reaction when 2 M H_2SO_4 and a solid-to-liquid ratio of 1:10 is used, which is the worst case, is presented in Appendix A.1. Regarding the calculations, all cathode materials are limiting agents that is, at these conditions, the concentration of acid is sufficient theoretically. Moreover,

the optimal solid-to-liquid ratio will be selected for further experiments, i.e. when current collectors are present during leaching (Chapter 4.3.2), when H_2O_2 is present (Chapters 4.4 and 4.5), and when black mass is leached (Chapter 4.6). Moreover, with the optimal solid-to-liquid ratio, aluminium foil and copper powder would also be added because of the ability to consume acid.

4.3.1 Effect of solid-to-liquid ratio

The solid-to-liquid ratio was varied as 1:100, 1:20, and 1:10 g/mL and the same amount of liquid was used (10 mL of 2 M H_2SO_4) to have an efficient mixing. The kinetic curves are plotted between leaching efficiency and leaching time for different desired solid-to-liquid ratios. Table 4.1 shows the theoretical volume of 2 M H_2SO_4 needed to leach different cathode materials based on stoichiometric ratios in the reaction equations and the actual volume of H_2SO_4 used in the leaching for different studied solid-to-liquid ratios. To compare, the numbers are divided by each cathode material weight.

Table 4.1: Theoretical of 2 M H_2SO_4 needed per gram of each cathode material and the amount of H_2SO_4 added at different solid-to-liquid ratios.

Cathode material	Theoretical volume needed of H_2SO_4 per cathode material weight (mL/g)	Added volume of H_2SO_4 per cathode material weight (ml/g)		
		1:100	1:20	1:10
LCO	7.65	100	20	10
NMC111	7.80			
NMC622	7.75			
NMC811	7.70			

According to Table 4.1, the volume of H_2SO_4 added is higher than the theoretical volume needed. It is expected that all leaching with these desired solid-to-liquid ratios is not limited by the leaching solution.

4.3.1.1 Leaching of LCO

In this section, the leaching of LCO was studied. Figures 4.10a and 4.10b show the leaching performances of lithium and cobalt between different solid-to-liquid ratios. Blue lines represent the kinetic curve when a solid-to-liquid of 1:100 g/mL was used. Orange and gray lines corresponds to 1:20 and 1:10 g/mL, respectively.

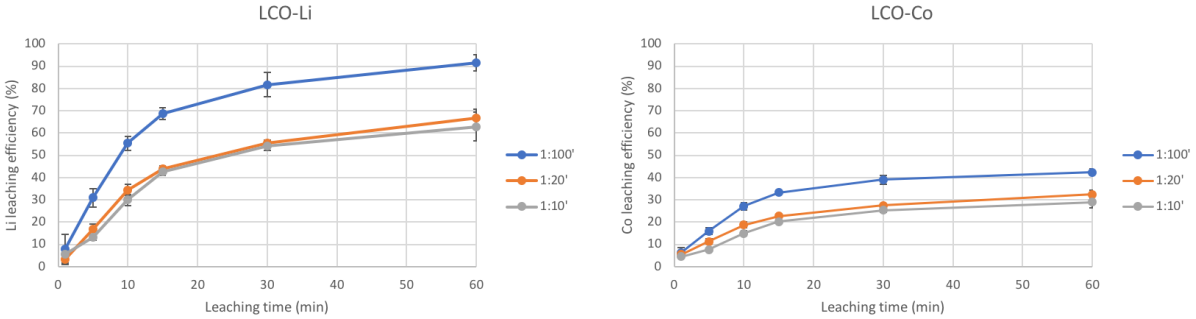

(a) Li leaching efficiency

(b) Co leaching efficiency

Figure 4.10: Leaching of LCO: Influence of solid-to-liquid ratio (reaction conditions: 2 M H_2SO_4, T=50°C, no H_2O_2, solid-to-liquid ratio of 1:10, 1:20, and 1:100 (10 mL solution)).

It can be seen from Figure 4.10a that the inclination of all three kinetic curves were the same. The leaching process occurred rapidly during the first 15 minutes and then slowed down. For all solid-to-liquid ratios, the lithium leaching efficiencies were not reaching certain values within 60 minutes leaching. It was expected that the ratio of 1:100 g/mL yielded the highest efficiency because there would be more free acid available for leaching. At solid-to-liquid ratios of 1:20 and 1:10, there was almost no difference in lithium leaching efficiency. The highest lithium leaching efficiencies were 91.5%, 66.7%, and 62.9% for solid-to-liquid ratios of 1:100, 1:20, and 1:10 g/mL, correspondingly.

In regard to Figure 4.10b, the same progression was also observed for all conditions that the cobalt leaching efficiency increased considerably during the first 15 minutes and then raised slightly. It can also be seen that the cobalt leaching efficiency at the ratio of 1:10 g/mL was similar to 1:20 g/mL and that these two ratios were inferior to that of 1:100 g/mL.

4.3.1.2 Leaching of NMC111

Figures 4.11a, 4.11b, 4.11c, and 4.11d review the influence of the solid-to-liquid ratio between 1:100, 1:20, and 1:10 on the leaching of NMC111.

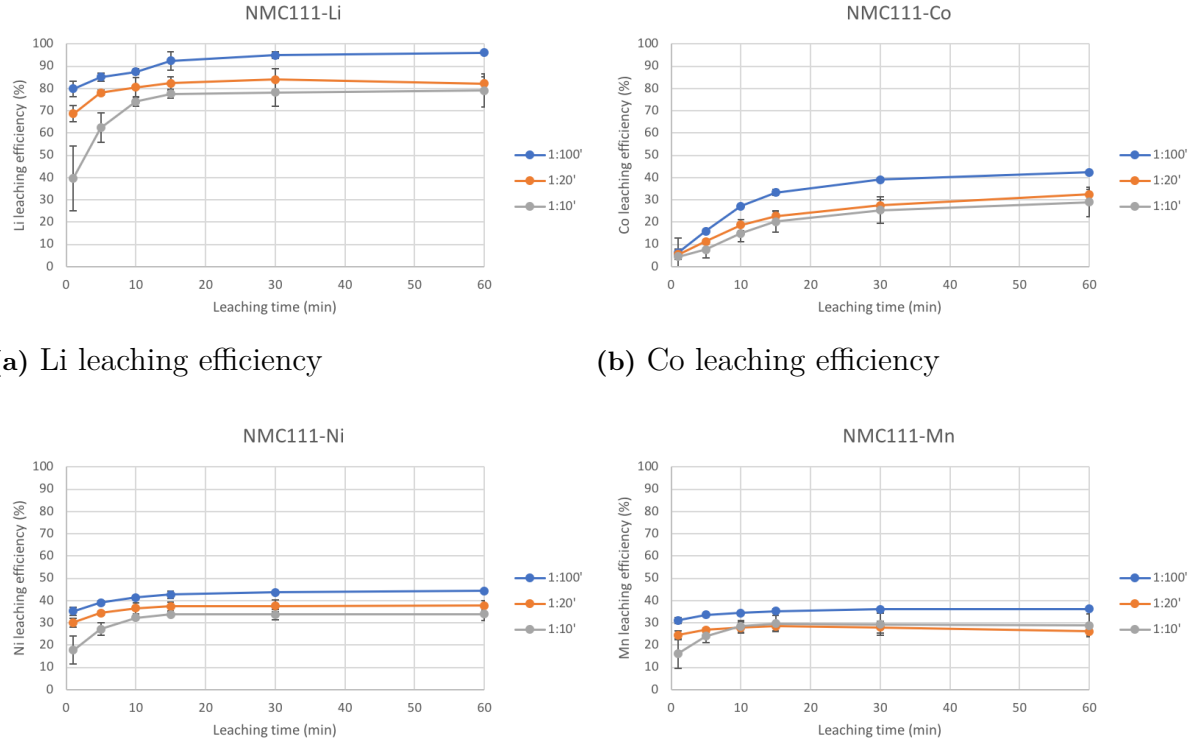

(a) Li leaching efficiency

(b) Co leaching efficiency

(c) Ni leaching efficiency

(d) Mn leaching efficiency

Figure 4.11: Leaching of NMC111: Influence of solid-to-liquid ratio (reaction conditions: 2 M H_2SO_4, T=50°C, no H_2O_2, solid-liquid ratio of 1:10, 1:20, and 1:100 (10 mL solution)).

The lithium leaching efficiency of the NMC111 is shown in Figure 4.11a. There was a very fast leaching initially especially for 1:100 and 1:20 (the increase after the initial 5 minutes of leaching was slower). Li was almost totally leached after 60 minutes leaching when using the solid-to-liquid ratio of 1:100. The difference in the maximum Li leaching efficiency between 1:10 and 1:20 was small.

According to Figure 4.11b, cobalt leaching efficiency in comparison of the three solid-to-liquid ratios is shown. The leaching trends were the same for all solid-to-liquid ratios. The curves raised throughout the investigated leaching time interval. It was clear that the ratio of 1:100 gave the highest cobalt leaching efficiency while the two other ratios gave pretty close values.

The nickel leaching efficiency when leaching NMC111 is illustrated in Figure 4.11c. It can be seen that faster initial leaching was obtained when the solid-to-liquid ratios of 1:100 and 1:20 were used. The curves were close to each other, i.e. small differences between the different ratios. The ratio of 1:10 gave the worst leaching efficiency; the maximum nickel leaching efficiency obtained after 60 minutes were 44.3%, 37.7%, and 33.9% from low to high solid-to-liquid ratio.

Figure 4.11d shows a plot of the manganese leaching efficiency. There was a faster leaching at the beginning and nothing much happened after 10–15 minutes for the solid-to-liquid ratios of 1:20 and 1:100. For the solid-to-liquid ratio of 1:100, the leaching curve overlapped with that of 1:20 after 10 minutes and small differences

between the solid-to-liquid ratios of 1:20 and 1:10 after 10-15 minutes were observed. The total manganese leaching efficiency after 60 minutes was still low (below 40%), therefore a reducing agent might be needed in order to obtain higher efficiency.

As a result, the kinetic curves of all solid-to-liquid ratios were parallel for all metals. The difference in the leaching efficiency between the three solid-to-liquid ratios was highest for lithium. The leaching efficiency was high for lithium (79-96%) and much lower for the other metals (<50%). However, the 1:100 ratio always gave the highest leaching efficiency while the solid-to-liquid ratios of 1:20 and 1:10 gave almost identical results.

4.3.1.3 Leaching of NMC622

Figures 4.12a, 4.12b, 4.12c, and 4.12d show the effect of the solid-to-liquid ratios 1:100, 1:20, and 1:10 g/mL on the leaching efficiency of NMC622.

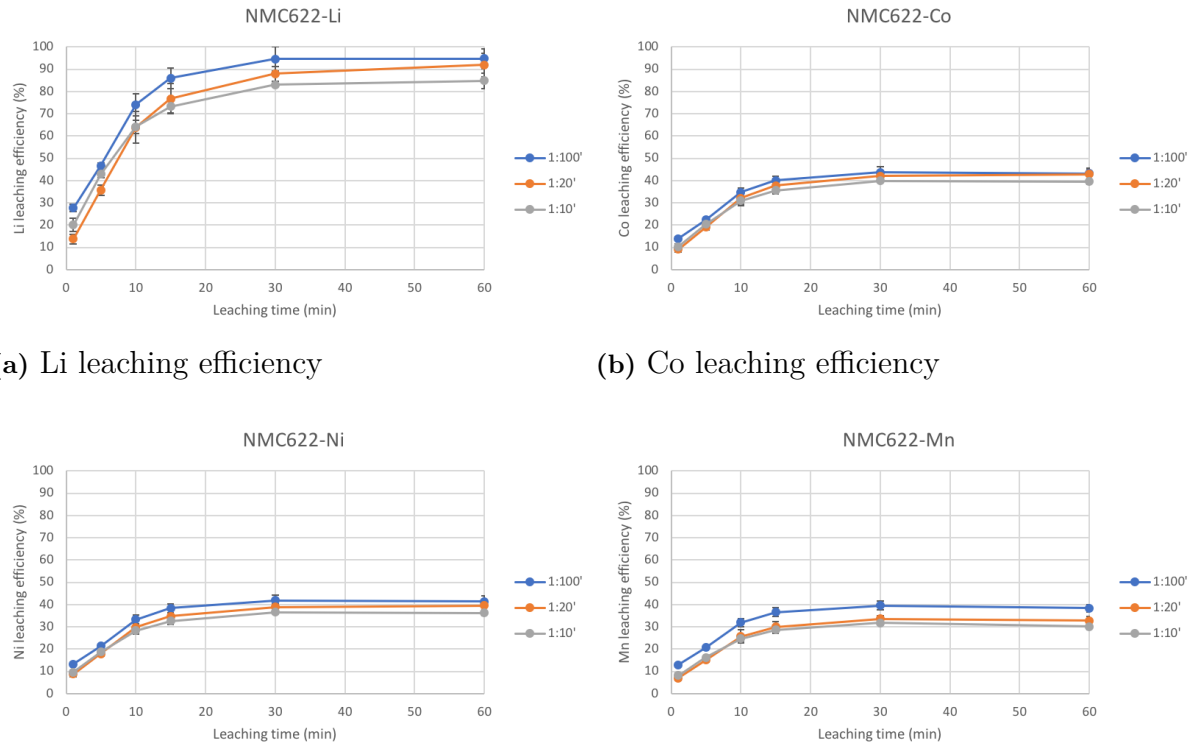

(a) Li leaching efficiency

(b) Co leaching efficiency

(c) Ni leaching efficiency

(d) Mn leaching efficiency

Figure 4.12: Leaching of NMC622: Influence of solid-to-liquid ratio (reaction conditions: 2 M H_2SO_4, T=50°C, no H_2O_2, solid-to-liquid ratio of 1:10, 1:20, and 1:100 (10 mL solution)).

Figure 4.12a illustrates the leaching kinetic curve of lithium over the time. Lithium leaching efficiencies increased the first 30 minutes and then reached an equilibrium. When the solid-liquid ratio was decreased, the lithium leaching efficiency was improved to some extent. Lithium was easily leached and the lithium

leaching efficiency was high for all solid-to-liquid ratios. Above 90% was achieved at the ratios of 1:100 and 1:20 g/mL and about 85% was reached at 1:10 g/mL.

In Figure 4.12b, the cobalt leaching efficiency is shown. The same trend was observed for all ratios and the value at every single point was close to each other. The cobalt leaching was only to a minor extent affected by the solid-to-liquid ratio; the maximum cobalt leaching efficiencies were 43.1%, 42.8%, and 39.6% at the ratio of 1:100, 1:20, and 1:10 g/mL, accordingly.

According to Figure 4.12c, at any solid-to-liquid ratios, the nickel was leached out continuously until it reached equilibrium after 30 minutes. The leaching performance was slightly better at lower solid-to-liquid ratio. The highest nickel leaching efficiency that could be reached were 41.1%, 39.5%, 36.2% when solid-to-liquid ratios of 1:100, 1:20, and 1:10 were used, respectively.

Figure 4.12d shows the manganese leaching efficiency of the NMC622 cathode material for the three desired solid-to-liquid ratios. It can be seen that a solid-to-liquid ratio of 1:100 yielded the highest manganese leaching performance while 1:20 and 1:10 gave about the same result. The maximum efficiencies were 38.3%, 32.8%, and 30.1% for 1:100, 1:20, and 1:10 g/mL, respectively.

4.3.1.4 Leaching of NMC811

The effect of varying solid-to-liquid ratio in term of metals' leaching efficiency is illustrated in Figures 4.13a, 4.13b, 4.13c, and 4.13d.

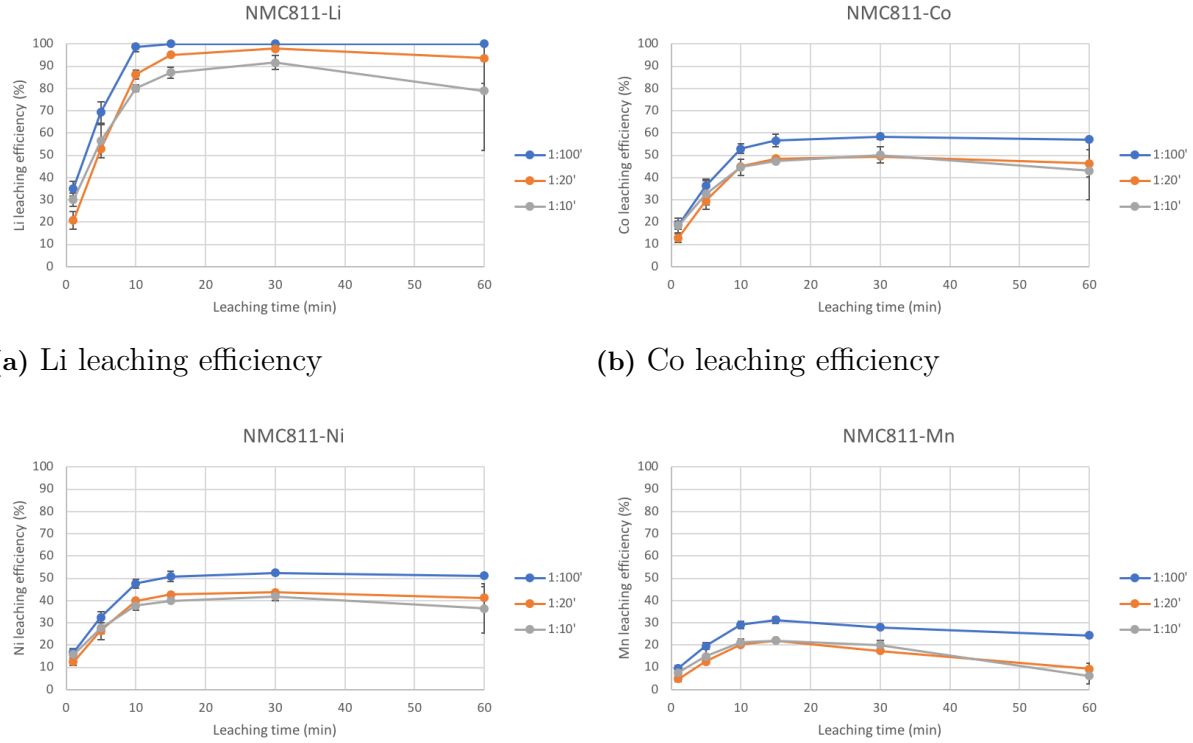

(a) Li leaching efficiency

(b) Co leaching efficiency

(c) Ni leaching efficiency

(d) Mn leaching efficiency

Figure 4.13: Leaching of NMC811: Influence of solid-to-liquid ratio (reaction conditions: 2 M H_2SO_4, T=50°C, no H_2O_2, solid-to-liquid ratio of 1:10, 1:20, and 1:100 (10 mL solution)).

Figure 4.13a is a plot of lithium leaching efficiencies in a comparison between three investigated solid-to-liquid ratios which are 1:100, 1:20, and 1:10. For NMC811, it was surprising that 100% of the Li was leached after 15 minutes, when using a solid-to-liquid ratio of 1:100, in the absence of a reducing agent. Moreover, the Li leaching efficiency for a ratio of 1:20 ratio was almost as good as for 1:100. For the highest solid-to-liquid ratio (1:10), the maximum leaching efficiency was obtained after 30 minutes.

The cobalt leaching performance, as seen in Figure 4.13b, increased considerably during the first 15 minutes and reached the maximum efficiency after 30 minutes and slightly dropped afterwards for the cases of 1:10 and 1:20 but for 1:100, it was stable. The cobalt leaching efficiency dropped when increasing solid-to-liquid ratio but there was no outstanding difference between 1:20 and 1:10.

For the nickel leaching efficiency as illustrated in Figure 4.13c, the leaching curve was the same as observed for cobalt leaching. The maximum nickel leaching efficiencies were 51.2%, 41.1%, and 36.5% for 1:100, 1:20, 1:10 g/mL, consequently.

In Figure 4.13d, the manganese leaching performance is shown, and an interesting trend was observed. The highest performance was measured after 15 minutes and the efficiency gradually dropped after that.

Therefore, it can be concluded that the effect of solid-to-liquid ratios on the leaching performance is the same for all cathode materials. Figure 4.14 shows a

comparison of the leaching efficiency for different cathode materials and solid-to-liquid ratios. The comparison is done at a leaching time of 60 minutes.

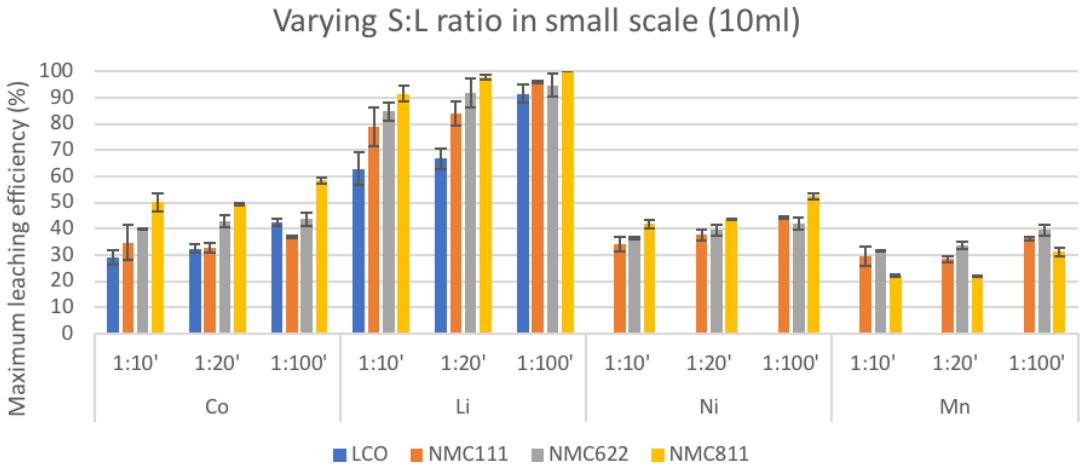

Figure 4.14: Leaching of all materials: Influence of solid-to-liquid ratio (reaction conditions: 2 M H_2SO_4, T=50°C, no H_2O_2, solid-to-liquid ratio of 1:100, 1:20, and 1:10, 10 mL solution, and 60 minutes leaching time).

The decreasing in solid-to-liquid ratio affected the leaching efficiency in all cathode material. Li was especially affected by the solid-to-liquid ratios for LCO whereas for the NMC cathode materials the difference was smaller and varying. It showed gradual improvement on other metals' leaching efficiencies for all cathode materials. Therefore, it can be concluded that the lowest solid-to-liquid ratio gives the highest leaching efficiency and that the difference between 1:20 and 1:10 was rather small but 1:20 was slightly better. Please note that this evaluation is done without a reducing agent present.

A solid-to-liquid ratio of 1:20 was selected for further experiments, when H_2O_2 was evaluated as reducing agent, to avoid a too concentrated leachate which is not suitable for the following solvent extraction process [68].

4.3.2 Effect of current collectors

With the selected solid-to-liquid ratio which was 1:20, aluminium foil and copper powder, which represent the current collectors, were added with an amount of 10% of the cathode's weight. The addition of Al and Cu foils is necessary since they can probably be presented in the black mass and also affect the leaching process. The leaching time in the following experiments was set to 45 minutes.

4.3.2.1 Leaching of LCO

Leaching of LCO with an addition of Cu and Al foils was studied in this section. The leaching efficiency when leaching with current collectors present was compared to the one without current collectors. Lithium and cobalt leaching efficiencies are

of an interest in the leaching of LCO and the results can be found in Figures 4.15a and 4.15b, respectively.

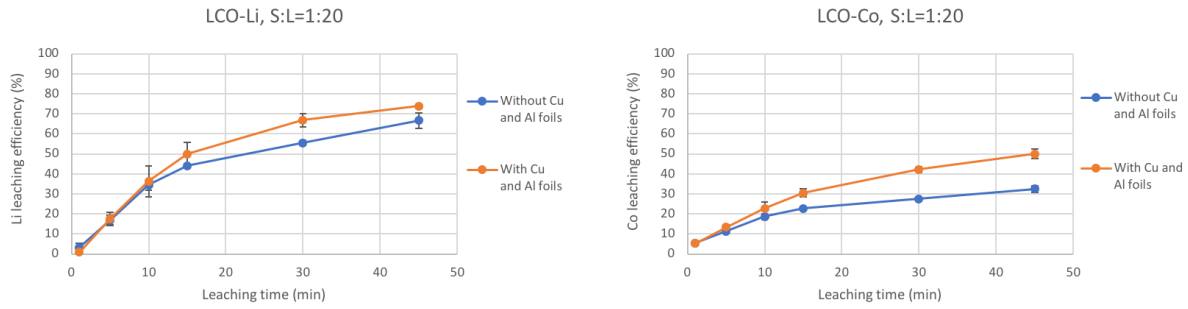

(a) Li leaching efficiency **(b)** Co leaching efficiency

Figure 4.15: Leaching of LCO: Influence of current collectors (reaction conditions: 2 M H_2SO_4, T=50°C, no H_2O_2, solid-to-liquid ratio of 1:20 (10 mL solution)).

According to Figure 4.15a, the blue line represents the kinetic curve of the leaching without current collectors and the orange line represents the kinetic curve of the leaching with current collectors. The maximum leaching performance of lithium was 73.8% after 45 minutes and a higher efficiency might be achieved since equilibrium was not reached. However, lithium is always the easiest element to be leached out whatever treatment condition due to the position of lithium; lithium loosely lies between molecular octahedral formed by cobalt and oxygen atoms in the LCO layer structure [69].

The leaching efficiency of cobalt is shown in Figure 4.15b. The maximum cobalt leaching efficiency was 49.9%. Cobalt leaching efficiency was much better when adding the current collectors.Cobalt leaching was more affected by the presence of Al and Cu foils than lithium leaching. The electrochemical potential is involved and affects the leaching reaction. Al and Cu have lower electrochemical potentials compared to cobalt. The standard electrode potentials are -1.662 V for Al, 0.34 V for Cu, and 1.82 V for Co. Due to their low values of electrochemical potential, Al and Cu could act as reducing agents in the leaching system. The leaching process is driven by galvanic interactions between current collectors (Al and Cu) and transition metal oxides that leads to a better dissolution of cobalt in the presence of current collectors. It reduces the oxidation state of Co and promote formation of $CoSO_4$.

4.3.2.2 Leaching of NMC111

The kinetic leaching curves of Li, Co, Ni, and Mn are illustrated in Figures 4.16a, 4.16b, 4.16c, and 4.16d, respectively.

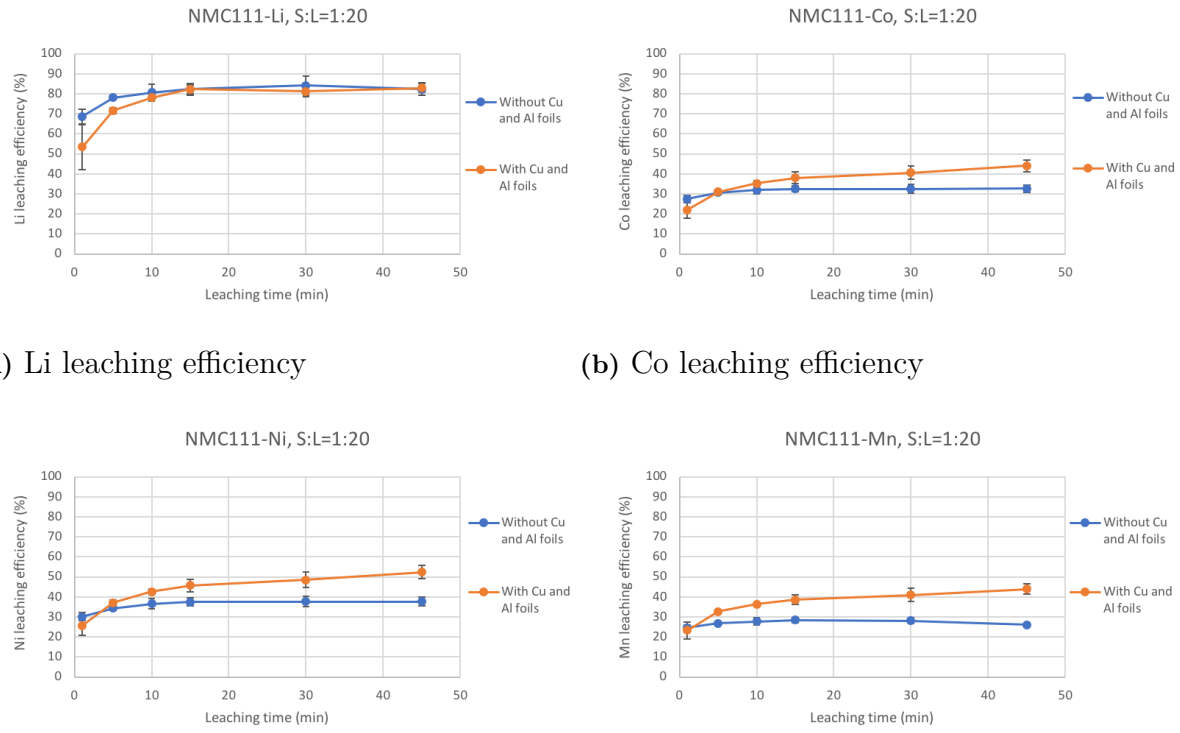

(a) Li leaching efficiency

(b) Co leaching efficiency

(c) Ni leaching efficiency

(d) Mn leaching efficiency

Figure 4.16: Leaching of NMC111: Influence of current collectors (reaction conditions: 2 M H_2SO_4, T=50°C, no H_2O_2, solid-to-liquid ratio of 1:20 (10 mL solution)).

As illustrated in Figure 4.16a, the leaching without Cu and Al foils could reach the maximum Li leaching efficiency faster than the leaching with Cu and Al foils. However, the leaching efficiency was almost the same, about 83-84%, at the end of leaching.

In the case of cobalt in Figure 4.16b, without an addition of Cu and Al foils, a slightly higher efficiency could be observed at the beginning and reached a constant value after 10 minutes. On the other hand, with an addition of current collectors, the efficiency was gradually increased and yielded better result. Roughly, the improvement was 35% when adding current collectors. This was due to the effect of changing to the preferred state of cobalt (Co^{2+}).

The same trend was also observed for Ni leaching as shown in Figure 4.16c. With the addition of current collectors, the maximum Ni leaching efficiency was 52.3% while the corresponding value without current collectors was 37.7%, i.e. an improvement with 39%.

Regarding Figure 4.16d, the trends of the Mn leaching kinetic curve looked the same as those of Co and Ni. With the addition of current collectors, the maximum Mn leaching efficiency was 44.0% whereas without current collectors it was 26.1% (an improvement of 69%). Therefore, the leaching of Mn was strongly affected by the presence of current collectors.

From all results, the addition of current collectors to the leaching of NMC111 could definitely promote the leaching efficiency except for lithium leaching. How-

ever, addition of current collectors affected mostly the cobalt, nickel, and manganese dissolution. The improvement was 35%, 39% ,and 69% for Co, Ni, and Mn, respectively. The Li was hardly affected by the reduction process unlike the Co, Ni, and Mn. For Li leaching, the influence from solid-to-liquid ratio, which was mentioned previously, was more important. The effect of current collectors on the lithium leaching is negligible since there is no change in oxidation state. However, a better dissolution of Co can promote the dissolution of Li. The leaching of nickel was also improved by about 39% because of liberation of other metals from the NMC111 structure. When the current collectors and cathode material are present together in the leaching solution, the metals from current collectors can function as reducing agents and promote the reduction of the metals as shown in the following equations.

$$Mn^{4+} + 2e^{-} \rightarrow Mn^{2+} \tag{4.1}$$

$$Co^{3+} + e^{-} \rightarrow Co^{2+} \tag{4.2}$$

The valence state 2+ is the stable state for Mn and Co in an aqueous solution. Their divalent forms are dissolved readily in H_2SO_4. Therefore, it is necessary to have reducing agents in the system to reduce the transition metal element from high valence states to low valence states to reach high leaching efficiencies.

4.3.2.3 Leaching of NMC622

Figures 4.17a, 4.17b, 4.17c, and 4.17d present the kinetic curves of NMC622 leaching for all leached metals, including Li, Co, Ni, and Mn, with an influence of an addition of current collectors.

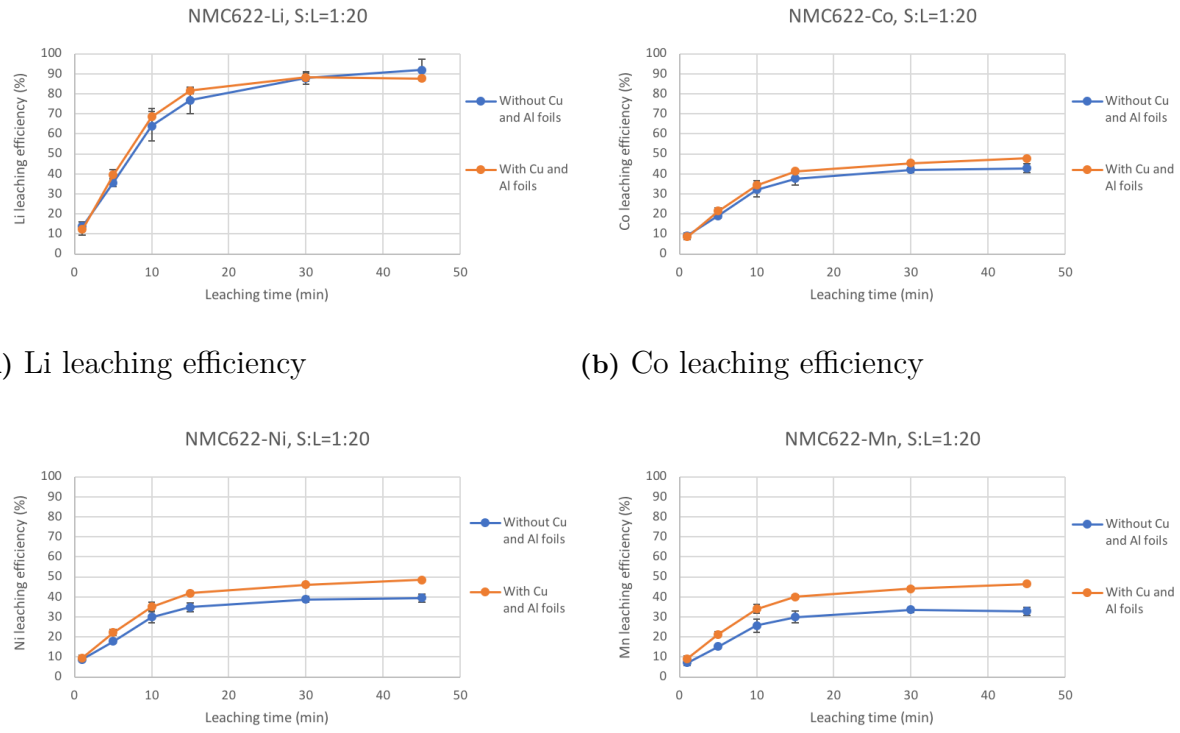

(a) Li leaching efficiency

(b) Co leaching efficiency

(c) Ni leaching efficiency

(d) Mn leaching efficiency

Figure 4.17: Leaching of NMC622: Influence of current collectors (reaction conditions: 2 M H_2SO_4, T=50°C, no H_2O_2, solid-to-liquid ratio of 1:20 (10 mL solution)).

Figure 4.17a shows the lithium leaching efficiency curves of NMC622 for both with and without an addition of current collectors. It can be seen that both curves have the same trend. Therefore, there was no clear improvement after an addition of Cu and Al foils on Li leaching efficiency.

According to Figure 4.17b, the same trend was observed for the cobalt leaching efficiency. When the current collectors were added, the cobalt leaching performance was slightly better compared to the leaching without current collectors but the difference was not large. The improvement was 11% when introducing current collectors.

In case of Ni, Figure 4.17c, it was clear that when introducing Cu and Al, the nickel leaching performance was better in every sampling. The maximum efficiencies were 48.4% and 39.5% with and without current collectors, respectively. The improvement was 22.6% when the current collectors were present.

As can be seen in Figures 4.17a-4.17d, the improvement when adding of Cu and Al was most pronounced for Mn compared to the other metals when leaching NMC622. The maximum Mn leaching efficiency increased with as much as 38%.

To sum up, the addition of Cu and Al foils led to higher leaching efficiency for Co, Ni, and Mn in NMC622. As mentioned above, due to the low electrochemical potentials, Cu and Al could function as reducing agents and by that promote metal dissolution as discussed above.

4.3.2.4 Leaching of NMC811

Figures 4.18a, 4.18b, 4.18c, and 4.18d present the leaching performance of NMC811 for all leached metals with and without the presence of current collectors.

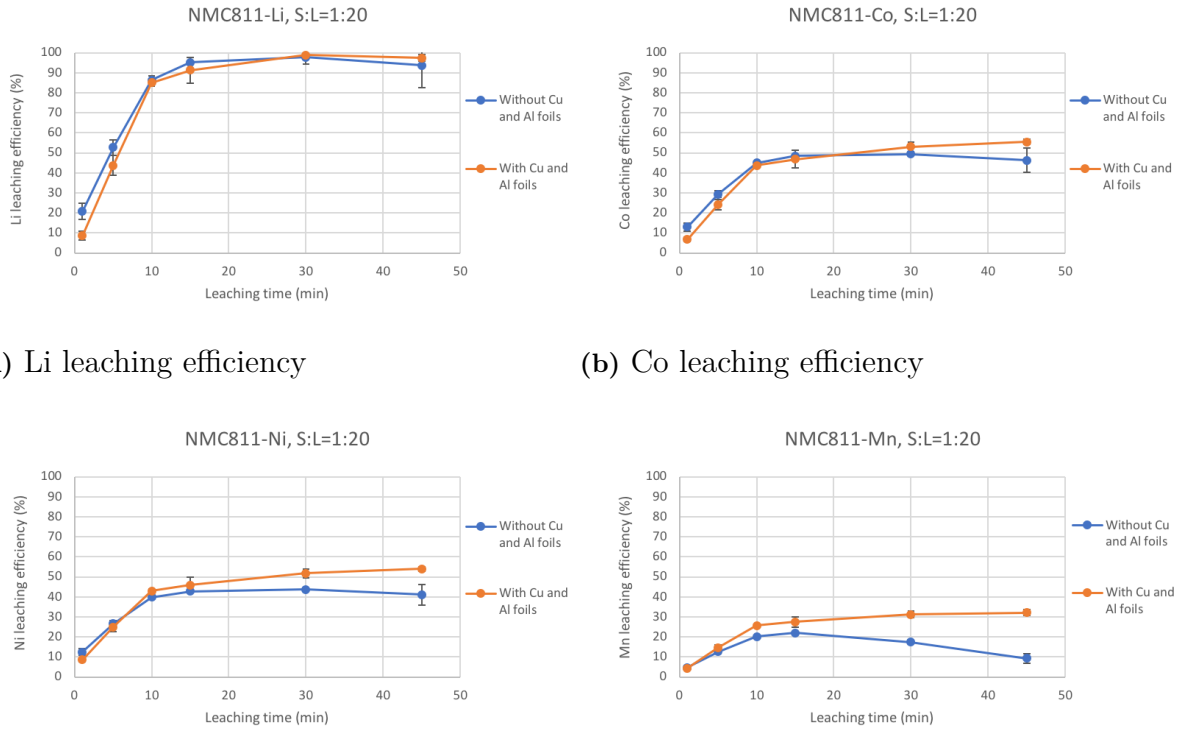

(a) Li leaching efficiency

(b) Co leaching efficiency

(c) Ni leaching efficiency

(d) Mn leaching efficiency

Figure 4.18: Leaching of NMC811: Influence of current collectors (reaction conditions: 2 M H_2SO_4, T=50°C, no H_2O_2, solid-to-liquid ratio of 1:20 (10 mL solution)).

As illustrated in Figure 4.18a, without an addition of Cu and Al, the maximum leaching was obtained after 30 minutes leaching and that the difference in leaching efficiency with or without current collectors was minor. The maximum lithium efficiencies for both conditions were 97.8% and 98.8% for without and with an addition of current collectors.

Figure 4.18b refers to cobalt leached performance of NMC811 leaching. It was shown that the leaching with the addition of current collectors improved the leaching efficiency after 30 minutes of leaching. As high as 55.4% of cobalt leaching efficiency could be achieved when Cu and Al were added into the solution while 49.4% was obtained when there was no Cu and Al present, i.e. an improvement of 12%.

Conforming to Figure 4.18c, nickel leaching efficiency was plotted against time. With an addition of Cu and Al foils, the efficiency was higher after 10 minutes. The improvement was 24% for nickel when introducing current collectors.

The largest improvement was clearly observed on manganese leaching that is presented in Figure 4.18d. As can be seen, an addition of Cu and Al foils made the leaching efficiency not to drop down like it was observed when the current collectors

were not added. The highest manganese leaching efficiencies were 22% and 32.1% for without and with an addition, consequently, i.e. an improvement of 46%. The concentration of Al and Cu in the final solution and the corresponding percent recovery are shown in Table 4.2 (where their initial concentrations were 500 ppm (10w/w% of each).

Table 4.2: Copper and aluminum concentration in leachate and percent recovery after 45 minutes leaching.

Cathode material	Cu conc. (ppm)	Cu leaching efficiency	Al conc. (ppm)	Al leaching efficiency
LCO	1.42	28.4%	0.71	14.3%
NMC111	0.09	1.9%	2.68	53.6%
NMC622	0.41	8.2%	0.52	10.4%
NMC811	0.63	12.6%	0.46	9.2%

As can be seen in Table 4.2, the final concentrations were rather low and the leaching efficiency was lower than for the other four desired valuable metals except for Al leaching in NMC111 (53.6%). It is clear that Cu and Al is not dissolved and stay undissolved in the leachate. Generally, in a real application, Al and Cu can be present in the leachate and then either solvent extraction or selective precipitation will be applied further to recover those metals.

To sum up, the addition of Cu and Al improved the leaching efficiency for both Li and Co (LCO), Co + Ni + Mn (NMC111), Co + Ni + Mn (NMC622), and Co + Ni + Mn (NMC811). Due to their low electrochemical potential of Cu and Al, they are able to lose electrons to cathode material that can promote them to be in the preferred state which can be easily leached out. The efficiency was high for Li but below 60% for Co, Ni, and Mn for all cathode materials. It is concluded that 2 M of sulfuric acid was able and sufficient to leach the desired metals. With as assist of a reducing agent, hydrogen peroxide, the leaching performance is expected to be better and higher leaching efficiency could be obtained.

4.4 Determination of optimal amount and addition strategy for hydrogen peroxide

4.4.1 Pre-determination of the optimal hydrogen peroxide volume percentage (%v/v) for different cathode materials

The theoretical amount of H_2O_2 needed for the leaching of each cathode material with a solid-to-liquid ratio of 1:20 g/mL was calculated (See Appendix A.2 for detailed calculations) and summarized in Table 4.3.

Table 4.3: The theoretical volume and concentration of H_2O_2 (59 wt%) needed.

Cathode material	Theoretical volume percentage of H_2O_2 needed (%v/v)	Theoretical amount of H_2O_2 needed (g/L)	Amount H_2O_2 needed per cathode material weight ($g_{H_2O_2}/g_{\text{cathode material}}$)
LCO	1.19	8.71	0.174
NMC111	0.40	2.93	0.059
NMC622	0.24	1.76	0.035
NMC811	0.12	0.87	0.017

Since the H_2O_2 consumption is expected to be higher than the stoichiometric amount because of the decomposition, the suitable volume of H_2O_2 for each cathode material was determined experimentally. In this pre-determining step, the leaching was done in small scale (10 mL of solution) and the H_2O_2 was added slowly (around $50-100$ μL at a time) until all cathode materials were totally dissolved. The actual amounts of H_2O_2 used in the leaching of the different cathode materials are shown in Table 4.4.

Table 4.4: The volume percentage of H_2O_2 needed to fully dissolve the cathode materials and addition time of H_2O_2 (59% of H_2O_2 was used).

Cathode material	Volume percentage of H_2O_2 used (%v/v)	H_2O_2 amount (g/L)	H_2O_2 adding time
LCO	7	51.3	0, 3, 6, 15, 22, 27, 35-minute
NMC111	3	22.0	0, 3, 6-minute
NMC622	4	29.3	0, 3, 6, 15-minute
NMC811	3	22.0	0, 3, 6-minute
LCO+10%w/w Cu, Al foils	8	58.6	0, 3, 6, 15, 22, 27, 35, 45-minute
NMC111+10%w/w Cu, Al foils	3	22.0	0, 3, 6-minute
NMC622+10%w/w Cu, Al foils	6	42.9	0, 3, 6, 15, 20, 27-minute
NMC811+10%w/w Cu, Al foils	3.5	25.6	0, 3, 6, 20-minute

The clear solutions with no precipitate were observed after leaching which can be seen from Figure 4.19 when there was no addition of copper and aluminum and Figure 4.20 when copper and aluminum were present.

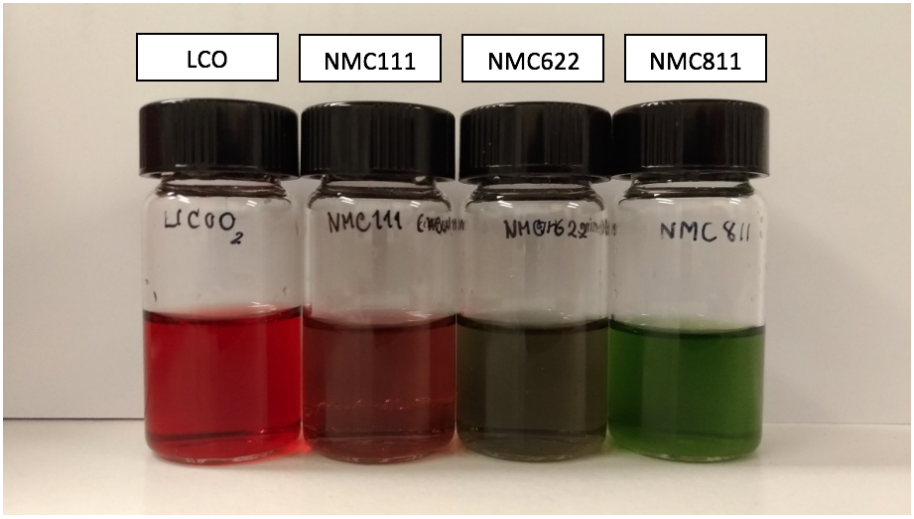

Figure 4.19: Leaching solution of all materials with no addition of current collectors (reaction conditions: 2 M H_2SO_4, T=50°C, with H_2O_2, solid-to-liquid ratio of 1:20 (10 mL solution)).

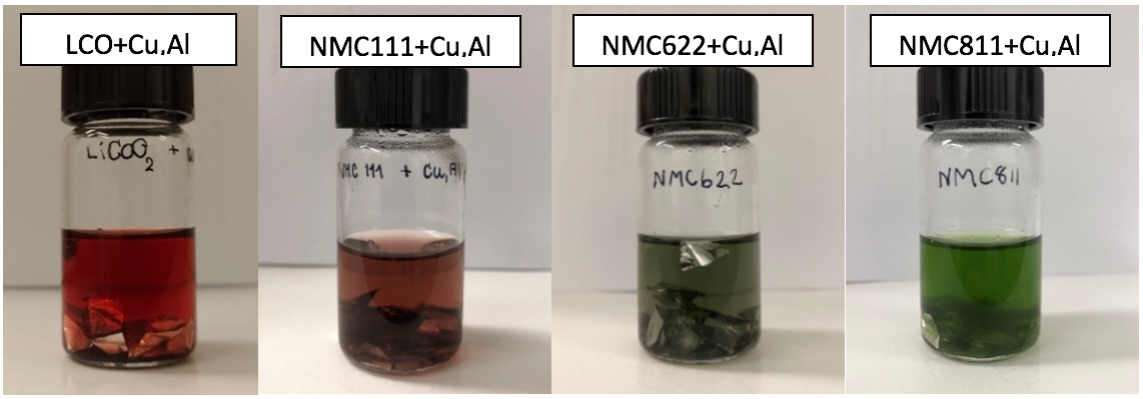

Figure 4.20: Leaching solution of all materials with an addition of current collectors (reaction conditions: 2 M H_2SO_4, T=50°C, with H_2O_2, solid-to-liquid ratio of 1:20 (10 mL solution)).

The residual amount of H_2O_2 was also measured by iodometric titration. Table 4.5 summarizes the amount of hydrogen peroxide left after the leaching of different cathode materials with and without addition of copper and aluminum foils.

Table 4.5: The residual amount of H_2O_2 after leaching for 60 minutes with and without current collectors.

Cathode material	Initial amount of H_2O_2 (g/L)	Residual amount of H_2O_2 (g/L)
LCO	51.3	45.1
NMC111	22.0	15.6
NMC622	29.3	19.6
NMC811	22.0	14.2
LCO+10%w/w Cu, Al foils	58.6	3.4
NMC111+10%w/w Cu, Al foils	22.0	0.6
NMC622+10%w/w Cu, Al foils	43.9	1.6
NMC811+10%w/w Cu, Al foils	25.6	2.9

From the results, the remaining amount of H_2O_2 when no copper and aluminum were added were still high after leaching (65-88% of the charged amount). The residual hydrogen peroxide was lower in the case when Cu and Al were added even if more hydrogen peroxide was added in most cases. The addition of copper and aluminum foils are likely to consume more hydrogen peroxide. The catalytic decomposition of H_2O_2 was promoted by copper [70].

4.4.2 Determination of the optimal addition strategy for hydrogen peroxide

All experiments were scaled up to 40 mL instead of 10 mL as in the pre-determining step to prevent the errors from sampling. The addition strategy for H_2O_2 was studied by adding all of the H_2O_2 at the beginning or by adding H_2O_2 on multiple occasions without altering the total amount of H_2O_2 charged. This was done to assess the leaching efficiency and amount of residual H_2O_2 after leaching. The volume percentage H_2O_2 and addition time were the same as in the previous part (see Table 4.4). For multiple addition, 400 µL of H_2O_2 was added each time until meeting the desired pre-determined amount. The sampling time was 1, 2, 3, 15, 30, and 60 minutes.

4.4.2.1 Determination of hydrogen peroxide consumption

According to Figures 4.21, 4.22, 4.23, and 4.24, the determination of remaining amount of H_2O_2 was done at 1-, 2-, 3-, 15-, 30- and 60-minute. In the case of adding all of the H_2O_2 once at the beginning, a rapid consumption occurred in the first 3 minutes of leaching where after the concentration decreased slowly until to a leaching time of 15 minutes.

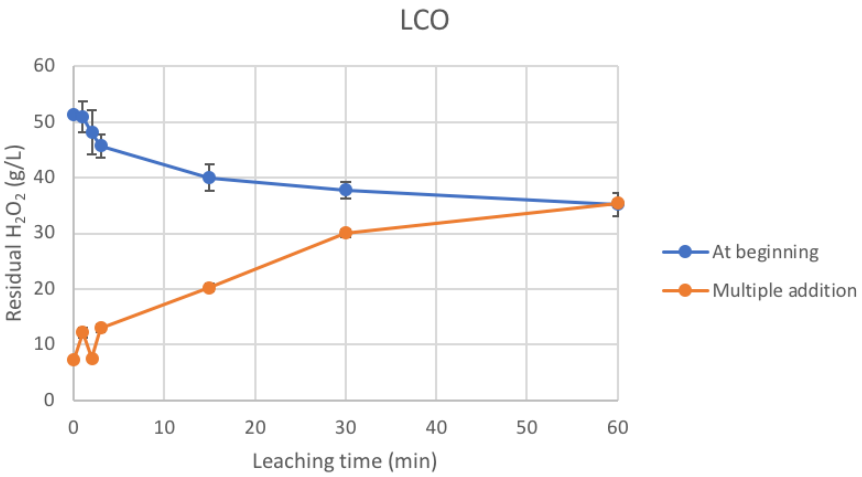

Figure 4.21: Leaching of LCO: Influence of H_2O_2 addition strategy on residual H_2O_2 concentration (reaction conditions: 2 M H_2SO_4, T=50°C, 7%v/v H_2O_2, solid-to-liquid ratio of 1:20 (40 mL solution)).

As shown in Figure 4.21, the initial concentration of H_2O_2 was 51.3 g/L when all H_2O_2 was added at once. During the first three minutes, the H_2O_2 concentration decreased rapidly to about 46 g/L (a decrease with about 11%) where after the H_2O_2 consumption leveled off and was 34 g/L after a leaching time of 60 minutes. On the other hand, when H_2O_2 was added at several occasions, a different consumption patterns was observed. Some variation in the amount of residual H_2O_2 occurred in the initial leaching phase, but after 30 minutes the residual H_2O_2 was approaching the same value for both addition strategies.

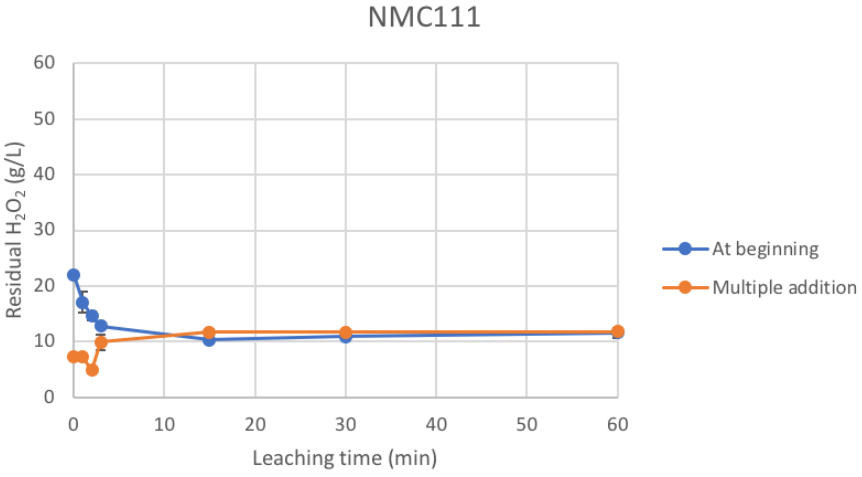

Figure 4.22: Leaching of NMC111: Influence of addition strategy on residual H_2O_2 concentration (reaction conditions: 2 M H_2SO_4, T=50°C, 3%v/v H_2O_2, solid-to-liquid ratio of 1:20 (40 mL solution)).

For NMC111 leaching with 3%v/v of hydrogen peroxide, the graph plotted

between the residual H_2O_2 and leaching time is shown as Figure 4.22. It can be seen that the leaching process occurred very rapidly in the beginning when all H_2O_2 was added at once. The first minute of leaching process, the concentration was reduced from 22 g/L to 17 g/L. The final residual H_2O_2 concentration was almost similar for both addition strategies (about 12 g/L).

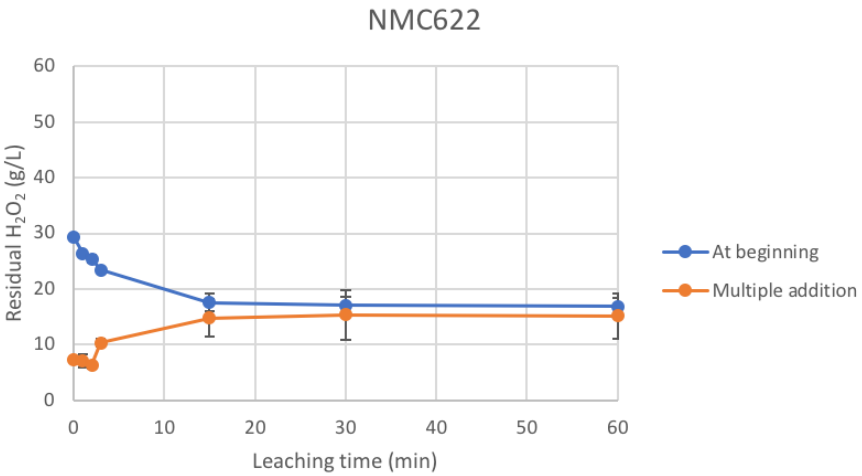

Figure 4.23: Leaching of NMC622: Influence of addition strategy on residual H_2O_2 concentration (reaction conditions: 2 M H_2SO_4, T=50°C, 4%v/v H_2O_2, solid-to-liquid ratio of 1:20 (40 mL solution)).

According to Figure 4.23, when H_2O_2 was added once at the beginning, the H_2O_2 was consumed very fast within 3 minutes. The concentration reduced from 29.3 to 23.4 g/L then gradually reduced and remained around 15 g/L for the rest of the leaching process. For the multiple addition, the concentration increased continuously and ended up with a value that was the same as when all H_2O_2 was added at the beginning. The difference between the two addition strategies was within the experimental error.

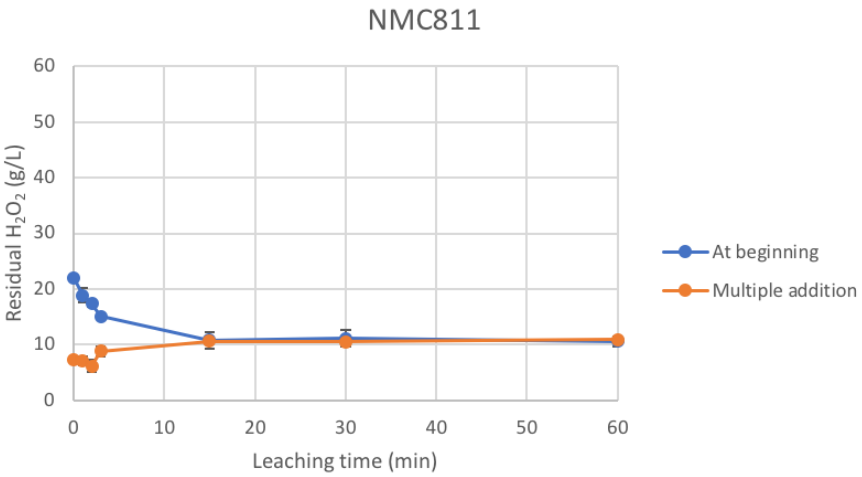

Figure 4.24: Leaching of NMC811: Influence of addition strategy on residual H_2O_2 concentration (reaction conditions: 2 M H_2SO_4, T=50°C, 3%v/v H_2O_2, solid-to-liquid ratio of 1:20 (40 mL solution)).

The residual amount of hydrogen peroxide during the leaching of NMC811 is shown in Figure 4.24. The initial concentration was 22.0 g/L and the final about 10.6 g/L, i.e. a consumption of 52%. During the first minute, the H_2O_2 concentration was reduced to 18.8 g/L when it was added once at the beginning. The remaining concentrations in solution were about 10 g/L for both addition strategies.

The kinetic consumption curve of H_2O_2 illustrated almost identical trend for all cathode materials regardless of addition strategy. After the initial reaction phase, the amount of residual H_2O_2 was stable for the remaining and maintained the same value for the whole leaching process. The leaching efficiency was also considered in order to select the best addition strategy of H_2O_2 when leaching LCO and NMC cathode materials (see below).

4.4.2.2 Determination of leaching efficiency

The following figures represent the kinetic leaching efficiency of different cathode materials along with the effect of addition strategy for hydrogen peroxide as mentioned in the previous section.

4.4.2.2.1 Leaching of LCO The kinetic leaching curve of LCO is illustrated in Figure 4.25 where the thick lines represent addition of H_2O_2 once at the beginning, thin lines represent multiple H_2O_2 additions, blue lines represent the kinetic curve for cobalt leaching whereas yellow lines represent the lithium leaching efficiency.

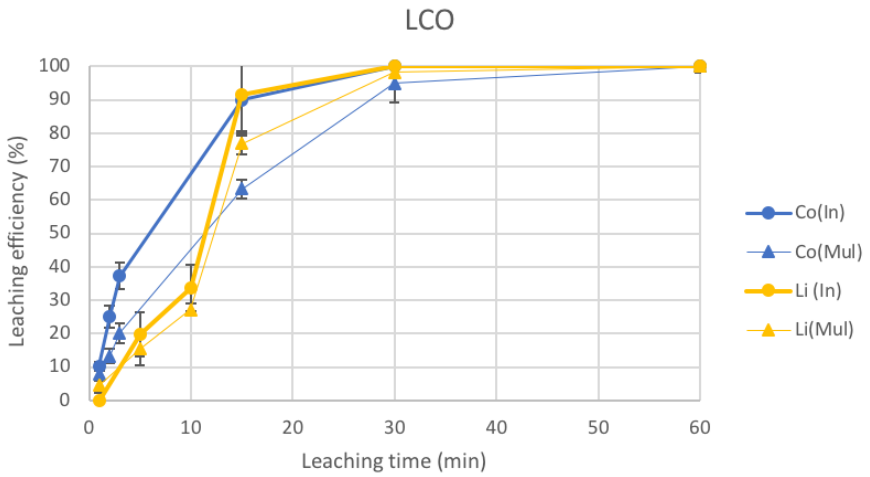

Figure 4.25: Leaching of LCO: Influence of H_2O_2 addition strategy on leaching efficiency (reaction conditions: 2 M H_2SO_4, T=50°C, 7%v/v H_2O_2, solid-to-liquid ratio of 1:20 (40 mL solution)). Thick lines represent the case when all H_2O_2 was added at the beginning and thin lines represent the case when H_2O_2 was added at multiple steps.

Identical trends could be observed for both addition strategies, i.e. that in the first 15-30 minutes the efficiency increased dramatically and reached constant values. The leaching was faster when all H_2O_2 was present from the beginning. However, at the end of the leaching process, 100% leaching efficiency could be obtained for all cases.

4.4.2.2.2 Leaching of NMC111 The leaching performance of NMC111 is illustrated in Figure 4.26. Cobalt leaching efficiency is represented as blue lines, lithium leaching efficiency is represented as yellow lines, manganese is represented as gray lines, and nickel is represented as orange lines.

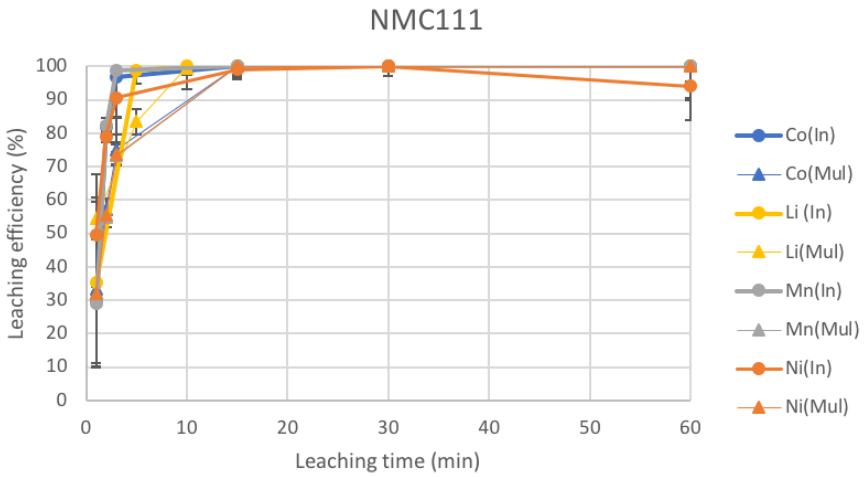

Figure 4.26: Leaching of NMC111: Influence of H_2O_2 addition strategy on leaching efficiency (reaction conditions: 2 M H_2SO_4, T=50°C, 3%v/v H_2O_2, solid-to-liquid ratio of 1:20 (40 mL solution)). Thick lines represent the case when all H_2O_2 was added at the beginning and thin lines represent the case when H_2O_2 was added at multiple steps.

According to Figure 4.26, in the case of initial addition of H_2O_2, the leaching efficiency raised sharply and almost touched the highest value after the first three minutes of leaching. A 100% leaching efficiency was achieved after 15 minutes leaching for both cases.

4.4.2.2.3 Leaching of NMC622 Figure 4.27 represent leaching efficiency of NMC622 as a function of leaching time.

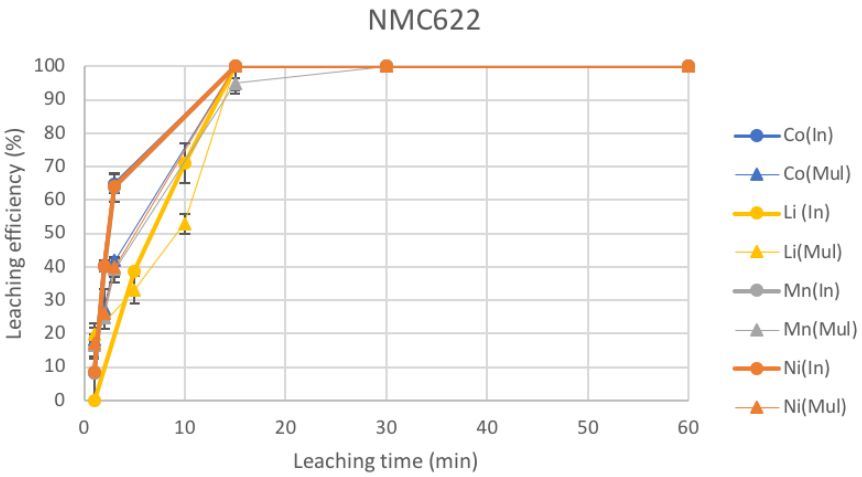

Figure 4.27: Leaching of NMC622: Influence of H_2O_2 addition strategy on leaching efficiency (reaction conditions: 2 M H_2SO_4 T=50°C, 4%v/v H_2O_2, solid-to-liquid ratio of 1:20 (40 mL solution)). Thick lines represent the case when all H_2O_2 was added at the beginning and thin lines represent the case when H_2O_2 was added at multiple steps.

The performance of cobalt, nickel, and manganese leaching was almost identical in each case except for lithium leaching. However, 100% leaching efficiency was reached after 30 minutes regardless of H_2O_2 addition strategy.

4.4.2.2.4 Leaching of NMC811 The NMC811 leaching performance is shown in Figure 4.28.

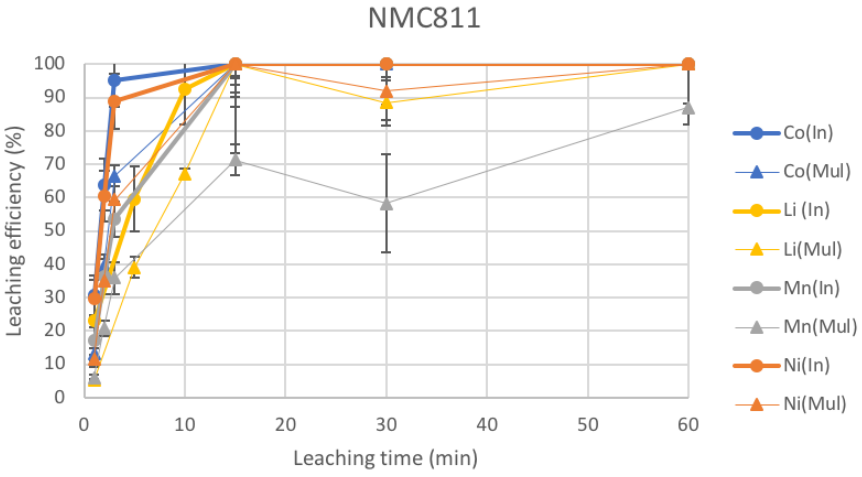

Figure 4.28: Leaching of NMC811: Influence of H_2O_2 addition strategy on leaching efficiency (reaction conditions: 2 M H_2SO_4, T=50°C, 3%v/v H_2O_2 solid-to-liquid ratio of 1:20 (40 mL solution)). Thick lines represent the case when all H_2O_2 was added at the beginning and thin lines represent the case when H_2O_2 was added at multiple steps.

Regarding Figure 4.28, some minor differences could be seen in the kinetic leaching curve which were the fluctuation in the leaching efficiency in the case of multiple addition of H_2O_2.

The leaching efficiency of all materials when H_2O_2 was added in the beginning reached the maximum leaching efficiency faster than for multiple addition of H_2O_2. All leached metal elements in all cathode materials reached 100% leaching efficiency except manganese in NMC811 that reached a leaching efficiency of about 87%. Therefore, in term of leaching efficiency, it was clear that addition of all H_2O_2 at the beginning gave a better result and this strategy was therefore selected.

4.5 Determination of leaching efficiency and hydrogen peroxide consumption in the presence of copper and aluminium foils

In this part of the study, when the four cathode materials were leached in the presence of H_2O_2, Cu, and Al, the conditions applied were based on the results from the previous studies. The operating conditions were 2 M H_2SO_4, solid-to-liquid ratio of 1:20, 50°C, and addition of all H_2O_2 from the beginning. A higher concentration of hydrogen peroxide is needed when introducing Cu and Al according to Chapter 4.4.1, the amount of hydrogen peroxide that was used when there was no Cu and Al added is not enough to dissolve all of the cathode materials in the leaching when Cu and Al exist. The volume percent (and g/L) of H_2O_2 needed is shown in Table 4.6. In this section, the experiments were scaled up to the scale of 40 mL liquid. 10%w/w of each Cu powder and Al foils were added, representing current collectors, in order to make the system more close to real industrial conditions.

Table 4.6: The amount of H_2O_2 used in the leaching trials (in %v/v and g/L).

Cathode material	Volume of H_2O_2 (%v/v)	H_2O_2 initial amount (g/L)
LCO	8.0	58.6
NMC111	3.0	22.0
NMC622	6.0	43.9
NMC811	3.5	25.6

4.5.1 Determination of hydrogen peroxide consumption

The graphs below are plotted between the residual amount of hydrogen peroxide and the leaching time for different materials comparing the H_2O_2 concentration in the leaching solution with and without copper and aluminum foils present. It is important to note that the initial concentration of H_2O_2 was not the same with and without Al and Cu in some cases, namely the leaching of LCO, NMC622, and NMC811. The point is to compare how the different cases consume H_2O_2.

4.5.1.1 Leaching of LCO

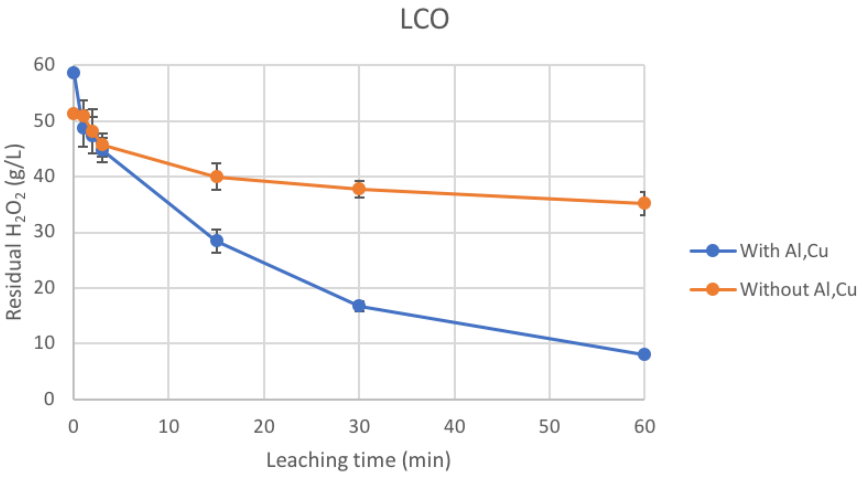

Figure 4.29: Leaching of LCO: Influence of the addition of current collectors on residual H_2O_2 concentration (reaction conditions: 2 M H_2SO_4, T=50°C, 7%v/v (no current collectors added) and 8%v/v (current collectors added) H_2O_2, solid-to-liquid ratio of 1:20 (40 mL solution)).

As illustrated in Figure 4.29, the amount of residual H_2O_2 concentration in the sample when Al and Cu were added was lower throughout the leaching process. The residual H_2O_2 concentration after a leaching time of 60 minutes was 35.2 g/L and 8.0 g/L when leaching without and with Cu and Al present, respectively. About 86% of initially charged H_2O_2 concentration was consumed in the case of addition Al and Cu.

4.5.1.2 Leaching of NMC111

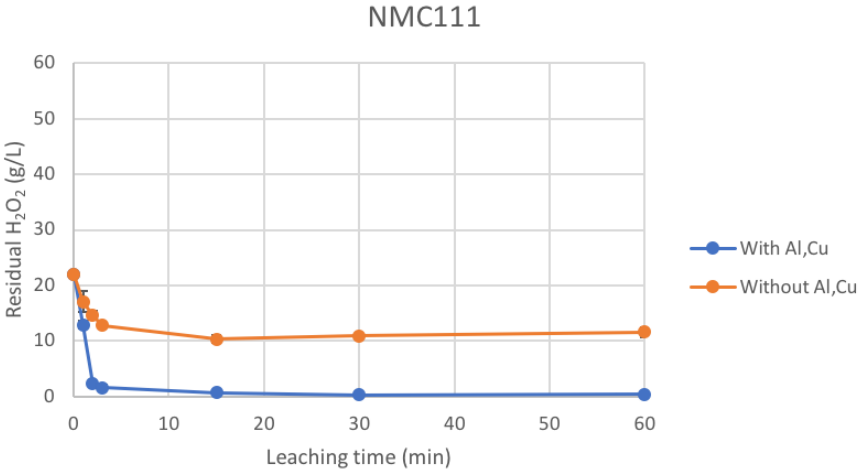

Figure 4.30: Leaching of NMC111: Influence of the addition of current collectors on residual H_2O_2 concentration (reaction conditions: 2 M H_2SO_4, T=50°C, 3%v/v H_2O_2 (both with and without current collectors), solid-to-liquid ratio of 1:20 (40 mL solution)).

In the case of NMC111 leaching, the residual H_2O_2 concentration was plotted against leaching time as shown in Figure 4.30. When the current collectors were present in the leaching solution, almost all of the added H_2O_2 was consumed after 15 minutes of leaching to a final concentration of about 0.4 g/L. The H_2O_2 consumption was lower for NMC111 than for LCO, i.e. 51 g/L was consumed for LCO and 22 g/L was consumed for NMC111 (in the presence of current collectors). Without Cu and Al present, H_2O_2 was consumed during the first 15 minutes of leaching to a final concentration of about 11 g/L. The H_2O_2 consumption in the presence of Cu and Al was much higher than without.

4.5.1.3 Leaching of NMC622

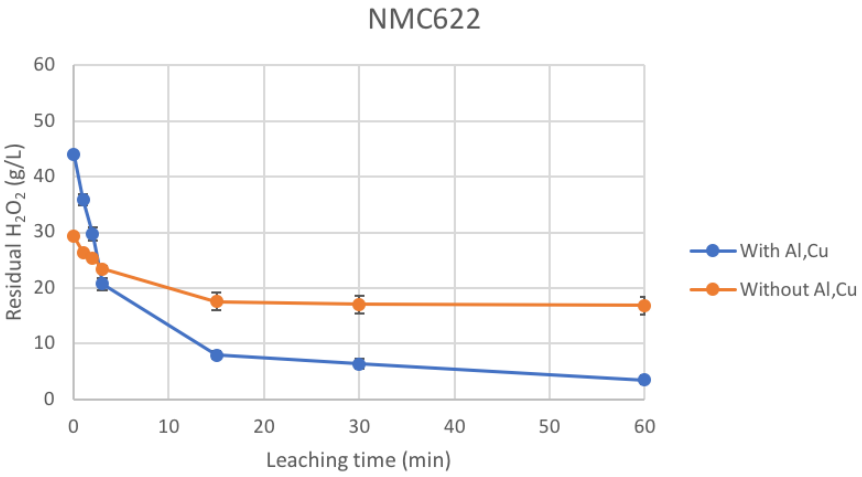

Figure 4.31: Leaching of NMC622: Influence of the addition of current collectors on residual H_2O_2 concentration (reaction conditions: 2 M H_2SO_4, T=50°C, 4%v/v (no current collectors added) and 6%v/v (current collectors added) H_2O_2, solid-to-liquid ratio of 1:20 (40 mL solution)).

According to Figure 4.31, with the presence of Al and Cu, the amount of H_2O_2 dropped drastically within the first three minutes of leaching to 20.7 g/L and still decreased readily after that. The amount of H_2O_2 present after 60 minutes was about 4 g/L and 17 g/L with and without current collectors present, respectively. About 90% and 42% of initial H_2O_2 amount were consumed in the case with and without current collectors present, respectively.

4.5.1.4 Leaching of NMC811

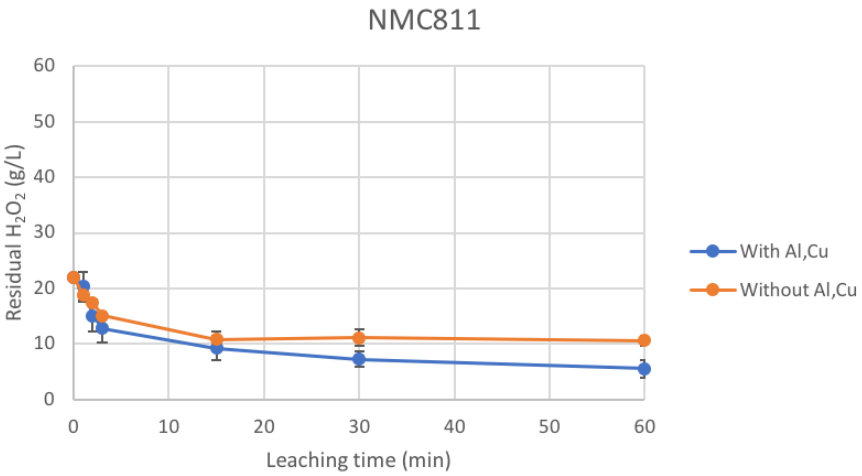

Figure 4.32: Leaching of NMC811: Influence of the addition of current collectors on residual H_2O_2 concentration (reaction conditions: 2 M H_2SO_4, T=50°C, 3%v/v (no current collectors added) and 3.5%v/v (current collectors added) H_2O_2, solid-to-liquid ratio of 1:20 (40 mL solution)).

On the other hand, in NMC811, the H_2O_2 concentration dropped from 22 g/L to about 13 g/L within the first three minutes and then slightly decreased until reached the final concentration which is 5.5 g/L when Al and Cu was present. The differences between the two cases were not extensive since about the same amount of H_2O_2 was added, somewhat higher H_2O_2 consumption if Cu and Al was present and that there still was H_2O_2 left after 60 minutes leaching (5.6–10.6 g/L).

Most of all, it was concluded that the addition of Al and Cu result in lower residual H_2O_2 concentration in the final solution. More H_2O_2 is consumed due to H_2O_2 decomposition induced by the current collectors (especially Cu). The residual H_2O_2 was less than 10 g/L in all leaching solutions with the presence of current collectors and was almost approaching zero in the NMC111 leaching solution.

4.5.2 Determination of leaching efficiency

The leaching efficiency was also of interest and examined in order to determine the performance when leaching in the presence of H_2O_2 and current collectors.

4.5.2.1 Leaching of LCO

The LCO leaching efficiency is illustrated in the figure below.

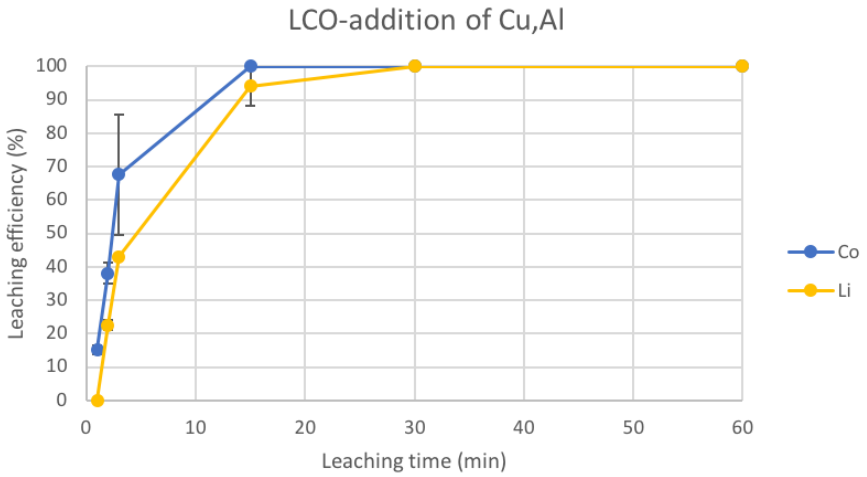

Figure 4.33: Leaching of LCO: Influence of the addition of current collectors on leaching efficiency (reaction conditions: 2 M H_2SO_4, T=50°C, 8%v/v H_2O_2, solid-to-liquid ratio of 1:20 (40 mL solution)).

In Figure 4.33, the LCO leaching performance was improved during the first 15 minutes when Cu and Al was present (cf. Figure 4.25) and a leaching efficiency of 100% was reached for both Co and Li within 30 minutes.

4.5.3 Leaching of NMC111

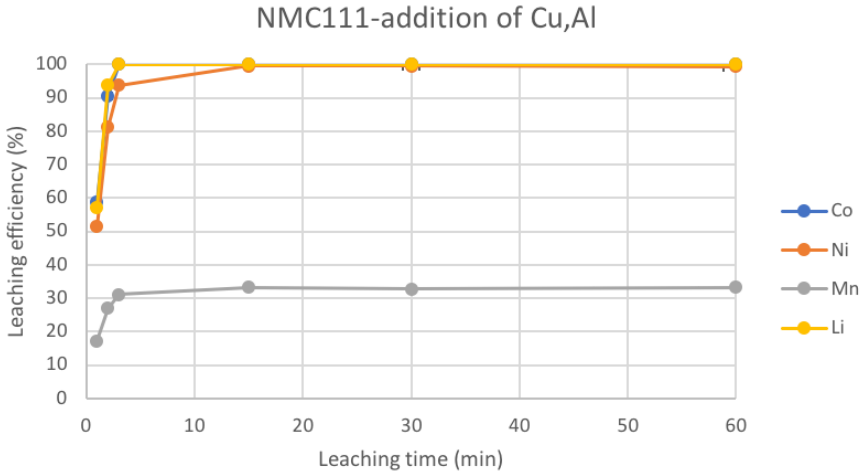

Figure 4.34: Leaching of NMC111: Influence of the addition of current collectors on leaching efficiency (reaction conditions: 2 M H_2SO_4, T=50°C, 3%v/v H_2O_2, solid-to-liquid ratio of 1:20 (40 mL solution)).

The leaching efficiency of Co, Ni, and Li in NMC111 raised steeply until reached the maximum performances as shown in Figure 4.34. On the contrary, the maximum leaching efficiency of Mn was only 32.9% which was significantly different from the

leaching without Cu and Al present as mentioned in the previous section, where a leaching efficiency of 100% was obtained.(cf. Figure 4.26)

4.5.4 Leaching of NMC622

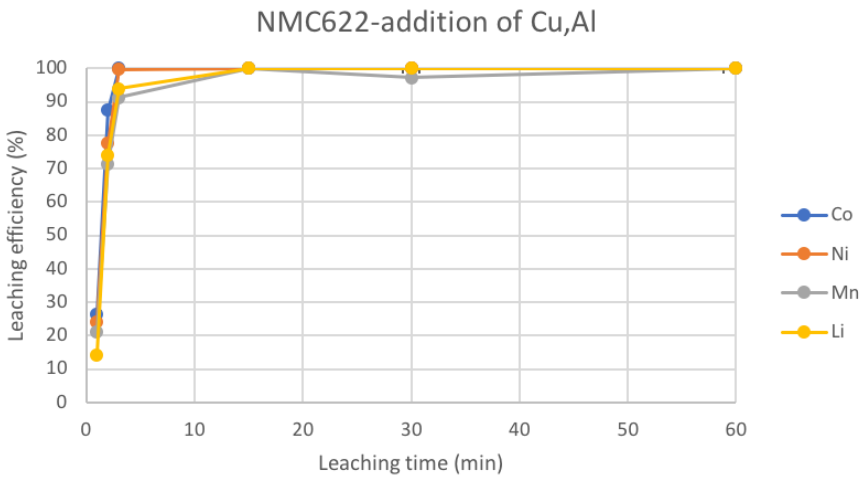

Figure 4.35: Leaching of NMC622: Influence of the addition of current collectors on leaching efficiency (reaction conditions: 2 M H_2SO_4, T=50°C, 6%v/v H_2O_2, solid-to-liquid ratio of 1:20 (40 mL solution)).

Figure 4.35 shows the leaching efficiency for NMC622, the leaching process was finished within 15 minutes. With the presence of both H_2O_2 and current collectors, there was no significant different in the leaching yield, but the total dissolution occurred faster with current collectors present (cf. Figure 4.27).

4.5.5 Leaching of NMC811

Figure 4.36 refers to a plot of metals' leaching efficiency of the leaching of NMC811.

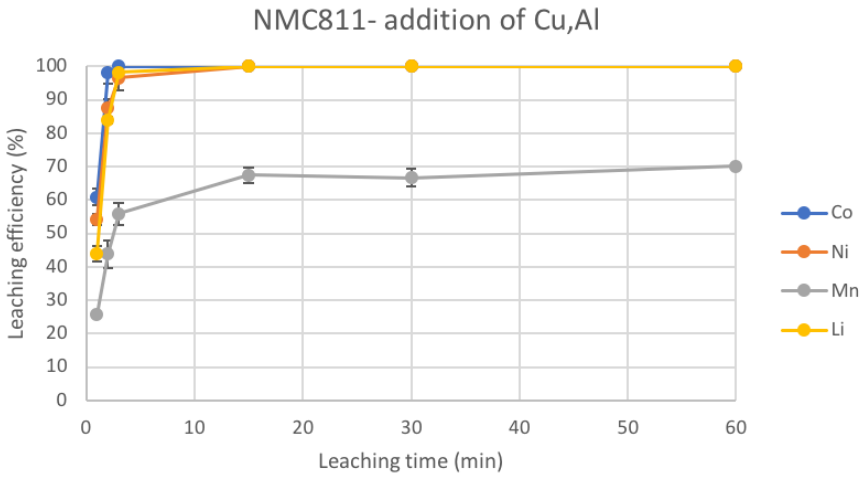

Figure 4.36: Leaching of NMC811: Influence of the addition of current collectors on leaching efficiency (reaction conditions: 2 M H_2SO_4, T=50°C, 3.5%v/v H_2O_2, solid-to-liquid ratio of 1:20 (40 mL solution)).

As a result, a leaching efficiency of 100% was reached within three minutes of leaching for Li, Co, and Ni whereas the maximum leaching efficiency reached for Mn was about 70% (after 60 minutes). The leaching efficiency of manganese in NMC811 varies among different conditions. The manganese leaching efficiencies were: 22% (without H_2O_2, Cu, Al), 32% (with Cu, Al), 87% (with H_2O_2, multiple), 100% (with H_2O_2, all at once), and 70% (with H_2O_2, all at once, Cu, Al) as shown in Figures 4.18d, 4.28, and 4.36. The presence of Cu can increase the rate of H_2O_2 decomposition. Therefore, a higher amount of H_2O_2 could have been needed in order to reach a leaching efficiency of 100% for all metals, especially for NMC111 and NMC811 where lower amounts of H_2O_2 was used compared to LCO and NMC622 as seen in Table 4.6.

4.6 Testing the optimal conditions on the real NMC cathode waste material

The black mass was provided by Volvo Cars, spent LiB cells from Volvo C30 Electric were mechanically treated and fractionated at Akkuser in Finland. The composition of black mass was analyzed and the results are shown in Table 4.7.

Table 4.7: Black mass composition

Element	%Weight
Li	3.43 ± 0.06
Co	10.51 ± 0.28
Ni	8.23 ± 0.15
Mn	7.49 ± 0.12
Cu	7.83 ± 0.06
Al	3.43 ± 0.00

The chemical composition of the spent Li-ion black mass was required to select the most suitable amount of H_2O_2. The black mass has the empirical formula as $Li_{1.087}Ni_{0.308}Mn_{0.300}Co_{0.392}O_2$ where the fraction of Ni, Mn, and Co is close to the NMC111 chemistry. Therefore, the optimal conditions previously obtained for NMC111 was used in the leaching experiments (in the presence of current collectors). The leaching efficiency and residual amount of H_2O_2 are illustrated in the following figures.

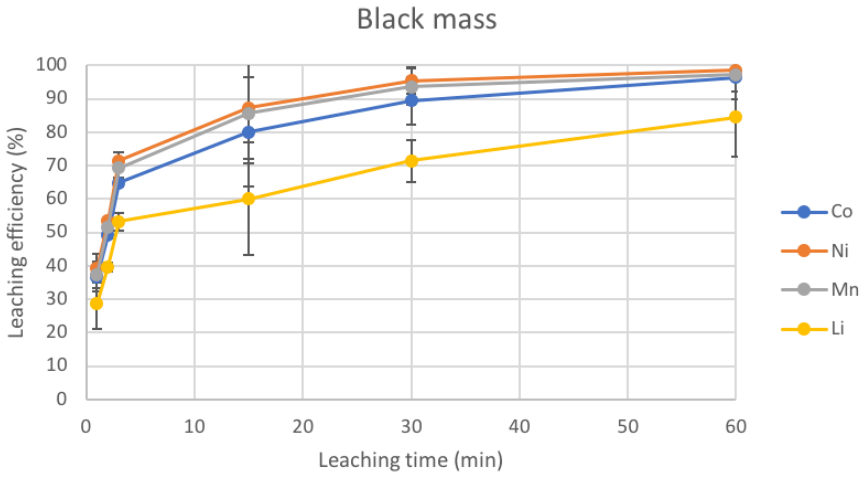

Figure 4.37: Leaching of black mass: Leaching efficiency (reaction conditions: 2 M H_2SO_4, T=50°C, 3%v/v H_2O_2, solid-to-liquid ratio of 1:20 (40 mL solution)).

According to the Figure 4.37, the leaching efficiency of Co, Ni, and Mn almost reached 100% after 60 minutes, whereas the Li leaching efficiency was around 85%. Some deviation from pure NMC111 can be observed as Li was not fully leached, Mn was almost totally leached and the leaching reaction was not as fast as observed for pure NMC111 (cf. Figure 4.34). However, all of the valuable elements can be leached effectively, especially manganese which a leaching efficiency increased from 33% in pure NMC111 (with H_2O_2, Cu, Al) to 97% in real spent NMC111.

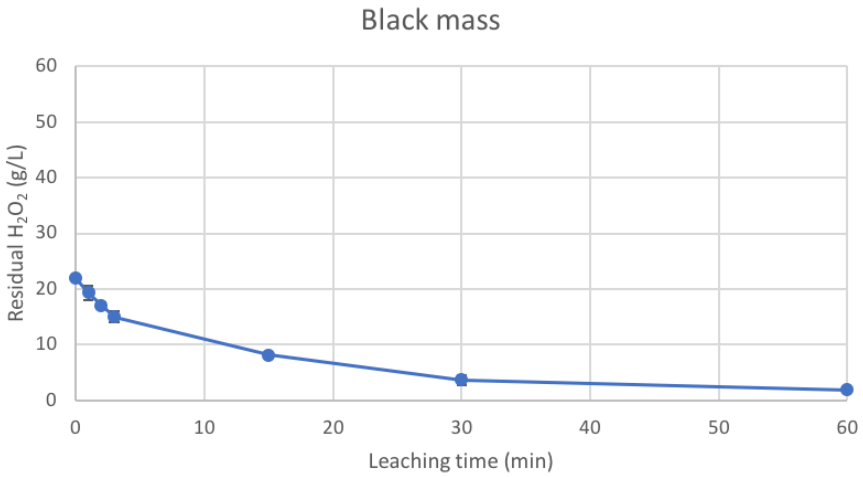

Figure 4.38: Leaching of black mass: Residual H_2O_2 concentration (reaction conditions: 2 M H_2SO_4, 3%v/v H_2O_2, solid-to-liquid ratio of 1:20 (40 mL solution)).

The residual H_2O_2 is shown in Figure 4.38. The kinetic curve decreased gradually and a very low concentration of H_2O_2 remained in the final solution (2.0 g/L). Since the amount of H_2O_2 was very low at the end of leaching process, an additional step to remove the residual H_2O_2 might not be necessary. To summarize, the charged H_2O_2 was used efficiently and the charge was appropriate for the further solvent extraction step.

5

Conclusion

In conclusion, the leaching performance without the addition of H_2O_2 and current collectors increased slightly when increasing the temperature in the interval 50°C to 60°C for the cathode materials LCO, NMC111, and NMC622, whereas the opposite was true for NMC811. Since the results were not significantly different, the lower temperature was judged to be preferable. Moreover, the leaching performance increased when the solid-to-liquid ratio was decreased because more free acid was available; a sulfuric acid concentration of 2 M was judged to be sufficient. A temperature of 50°C and solid-to-liquid ratio of 1:20 (40 mL of leaching solution) were chosen as the best suitable condition for the following experiments. In addition, the presence of Cu and Al current collectors had a positive effect on the leaching efficiency due to low electrochemical potentials, i.e. Cu and Al could act as reducing agents and enhance the leaching process. Co, Ni, and Mn were clearly affected by having Cu and Al present in the leaching solution. Moreover, all metal leaching was promoted by the effect of mixing especially Li.

The effect of addition of hydrogen peroxide (as reducing agent) on the leaching efficiency was investigated for the four cathode materials. The optimal H_2O_2 concentration in the leaching solution was a function of cathode material and the presence of Cu and Al current collectors. In larger scale, all metals in pure NMC111, NMC622, and NMC811 can be completely leached within 15 minutes if H_2O_2 is present but for LCO, 60 minutes of leaching was required. It was evident that the leaching efficiency for Co, Ni, and Mn was strongly improved when H_2O_2 was present during leaching whereas the Li leaching efficiency was not promoted to any great extent. This is because the lithium's valence state was not changed by H_2O_2. The addition strategy of H_2O_2 was also studied by adding all of the H_2O_2 at the beginning of leaching or adding H_2O_2 at multiple occasions during the leaching process without altering the total amount of H_2O_2 charged. The addition strategy did not affect the amount of H_2O_2 that was consumed or the leaching efficiency; the maximum leaching efficiency was, however, reached faster when all of the H_2O_2 was charged at the beginning. Therefore, initial addition of H_2O_2 is recommended.

The proposed optimum NMC111 conditions (50°C, solid-to-liquid ratio of 1:20, 3%v/v H_2O_2) was used when leaching black mass from spent Volvo C30 Electric Li-ion batteries having a composition of $Li_{1.087}Ni_{0.308}Mn_{0.300}Co_{0.392}O_2$. As a result, hydrogen peroxide was almost completely consumed and 100% of Co, Ni, and Mn efficiencies could be reached, whereas the maximum leaching efficiency for Li was about 85%.

The results from this master thesis could be a valuable contribution to the area of spent Li-ion battery recycling especially on the sulfuric acid leaching process

assisted by hydrogen peroxide. By employing the proposed optimum conditions (50°C, solid-to-liquid ratio of 1:20, efficient mixing, optimal charge of H_2O_2 as a function of cathode material), a high metal recovery rate could be achieved.

References

[1] Jianqiang Kang et al. "Comparison of comprehensive properties of Ni-MH (nickel-metal hydride) and Li-ion (lithium-ion) batteries in terms of energy efficiency". In: *Energy* 70 (2014), pp. 618–625. ISSN: 0360-5442.

[2] Christophe Pillot. "The rechargeable battery market and main trends 2014–2025". In: *31st International Battery Seminar & Exhibit*. 2015.

[3] Yemeserach Mekonnen, Aditya Sundararajan, and Arif I Sarwat. "A review of cathode and anode materials for lithium-ion batteries". In: *SoutheastCon 2016*. IEEE. 2016, pp. 1–6.

[4] X. Chen et al. "An overview of lithium-ion batteries for electric vehicles". In: *2012 10th International Power Energy Conference (IPEC)*. Dec. 2012, pp. 230–235. DOI: 10.1109/ASSCC.2012.6523269.

[5] US Geological Survey & Orienteering S and US Geological Survey. *Mineral Commodity Summaries, 2019*. Government Printing Office, 2019.

[6] Rabeeh Golmohammadzadeh, Fariborz Faraji, and Fereshteh Rashchi. "Recovery of lithium and cobalt from spent lithium ion batteries (LIBs) using organic acids as leaching reagents: A review". In: *Resources, Conservation and Recycling* 136 (2018), pp. 418–435. ISSN: 0921-3449. DOI: https://doi.org/10.1016/j.resconrec.2018.04.024. URL: http://www.sciencedirect.com/science/article/pii/S0921344918301629.

[7] Cobalt Institute. *Critical Raw Material*. Apr. 2020. URL: https://www.cobaltinstitute.org/critical-raw-material.html.

[8] *Cobalt2010-2020 Data: 2021-2022 Forecast: Price: Quote: Chart: Historical*. URL: https://tradingeconomics.com/commodity/cobalt.

[9] M.C. McManus. "Environmental consequences of the use of batteries in low carbon systems: The impact of battery production". In: *Applied Energy* 93 (2012). (1) Green Energy; (2)Special Section from papers presented at the 2nd International Enery 2030 Conf, pp. 288–295. ISSN: 0306-2619.

[10] Helen Lewis. *Lithium-ion battery consultation report*. 2016.

[11] "Waste statistics - recycling of batteries and accumulators". In: *Eurostat Statistics Explained* (2019).

[12] Martin Winter and Ralph J. Brodd. "What Are Batteries, Fuel Cells, and Supercapacitors?" In: *Chemical Reviews* 104.10 (2004). PMID: 15669155, pp. 4245–4270. DOI: 10.1021/cr020730k.

[13] M Endo et al. "Recent development of carbon materials for Li ion batteries". In: *Carbon* 38.2 (2000), pp. 183–197.

[14] The Authoritative Voice of the Portable Battery Industry. "Product information,primary and recharegeable batteries". In: (2015). URL: https://www.

epbaeurope.net/wp-content/uploads/2016/12/EPBA_Product-Information_10112015.pdf.

[15] Sascha Nowak and Martin Winter. "Elemental analysis of lithium ion batteries". In: *J. Anal. At. Spectrom.* 32 (10 2017), pp. 1833–1847.

[16] Jun Lu et al. "High-performance anode materials for rechargeable lithium-ion batteries". In: *Electrochemical Energy Reviews* 1.1 (2018), pp. 35–53.

[17] Kiyoung Lee, Anca Mazare, and Patrik Schmuki. "One-dimensional titanium dioxide nanomaterials: nanotubes". In: *Chemical reviews* 114.19 (2014), pp. 9385–9454.

[18] PLSG Poizot et al. "Nano-sized transition-metal oxides as negative-electrode materials for lithium-ion batteries". In: *Nature* 407.6803 (2000), p. 496.

[19] M. Stanley Whittingham. "Materials Challenges Facing Electrical Energy Storage". In: *MRS Bulletin* 33.4 (2008), pp. 411–419. DOI: 10.1557/mrs2008.82.

[20] Narjes Kheirabadi and Azizollah Shafiekhani. "Graphene/Li-ion battery". In: *Journal of Applied Physics* 112.12 (2012), p. 124323.

[21] *Comparison of Lithium-Ion Battery Cathode Materials and the Internal Stress Development*. Vol. Volume 4: Energy Systems Analysis, Thermodynamics and Sustainability; Combustion Science and Engineering; Nanoengineering for Energy, Parts A and B. ASME International Mechanical Engineering Congress and Exposition. Nov. 2011, pp. 1685–1694.

[22] Longlong Wang et al. "Reviving lithium cobalt oxide-based lithium secondary batteries-toward a higher energy density". In: *Chemical Society Reviews* 47.17 (2018), pp. 6505–6602.

[23] Isidor Buchmann et al. *Batteries in a portable world: a handbook on rechargeable batteries for non-engineers*. Cadex Electronics Richmond, 2001.

[24] K Mizushima et al. "LixCoO2 (0< x 1): A new cathode material for batteries of high energy density". In: *Solid State Ionics* 3 (1981), pp. 171–174.

[25] E Plichta et al. "An improved Li/Li x CoO2 rechargeable cell". In: *Journal of the Electrochemical Society* 136.7 (1989), pp. 1865–1869.

[26] Ermete Antolini. "LiCoO2: formation, structure, lithium and oxygen nonstoichiometry, electrochemical behaviour and transport properties". In: *Solid State Ionics* 170.3 (2004), pp. 159–171. ISSN: 0167-2738.

[27] HF Gibbard. "High temperature, high pulse power lithium batteries". In: *Journal of Power Sources* 26.1-2 (1989), pp. 81–91.

[28] Christian M Julien et al. "Comparative issues of cathode materials for Li-ion batteries". In: *Inorganics* 2.1 (2014), pp. 132–154.

[29] Roland Jung et al. "Chemical versus electrochemical electrolyte oxidation on NMC111, NMC622, NMC811, LNMO, and conductive carbon". In: *The journal of physical chemistry letters* 8.19 (2017), pp. 4820–4825.

[30] Tsutomu Ohzuku and Yoshinari Makimura. "Layered Lithium Insertion Material of LiCo1/3Ni1/3Mn1/3O2 for Lithium-Ion Batteries". In: *Chemistry Letters - CHEM LETT* 1 (Jan. 2001), pp. 642–643. DOI: 10.1246/cl.2001.642.

[31] Targray Technology International Inc. *NMC Powder (LiNiMnCoO2) Lithium Nickel Manganese Cobalt Oxide Cathode for Li-ion Batteries*. URL: https://www.targray.com/li-ion-battery/cathode-materials/nmc (visited on 01/31/2020).

[32] Sankar Dasgupta and James K Jacobs. *Current collector for lithium ion battery*. US Patent 5,547,782. Aug. 1996.

[33] Xiaosong Huang. "Separator technologies for lithium-ion batteries". In: *Journal of Solid State Electrochemistry* 15.4 (2011), pp. 649–662.

[34] Rajagopalan Kannan et al. "Analysis of the separator thickness and porosity on the performance of Lithium-Ion batteries". In: *International Journal of Electrochemistry* 2018 (2018).

[35] Xiaosong Huang and Jonathon Hitt. "Lithium ion battery separators: Development and performance characterization of a composite membrane". In: *Journal of Membrane Science* 425-426 (2013), pp. 163–168. ISSN: 0376-7388.

[36] Jolanta Świątowska and Philippe Barboux. "Chapter 4 - Lithium Battery Technologies: From the Electrodes to the Batteries". In: *Lithium Process Chemistry*. Ed. by Alexandre Chagnes and Jolanta Świątowska. Amsterdam: Elsevier, 2015, pp. 125–166. ISBN: 978-0-12-801417-2.

[37] Bruno Scrosati. "Recent advances in lithium ion battery materials". In: *Electrochimica Acta* 45.15 (2000), pp. 2461–2466. ISSN: 0013-4686.

[38] Steven E Sloop, John B Kerr, and Kim Kinoshita. "The role of Li-ion battery electrolyte reactivity in performance decline and self-discharge". In: *Journal of Power Sources* 119-121 (2003). Selected papers presented at the 11th International Meeting on Lithium Batteries, pp. 330–337. ISSN: 0378-7753.

[39] George E Blomgren. "Electrolytes for advanced batteries". In: *Journal of Power Sources* 81-82 (1999), pp. 112–118. ISSN: 0378-7753.

[40] Sheng Shui Zhang. "A review on electrolyte additives for lithium-ion batteries". In: *Journal of Power Sources* 162.2 (2006). Special issue including selected papers from the International Power Sources Symposium 2005 together with regular papers, pp. 1379–1394. ISSN: 0378-7753.

[41] Perla B Balbuena and Yixuan Wang. *Lithium-ion batteries: solid-electrolyte interphase*. Imperial college press, 2004.

[42] Seong Jin An et al. "The state of understanding of the lithium-ion-battery graphite solid electrolyte interphase (SEI) and its relationship to formation cycling". In: *Carbon* 105 (2016), pp. 52–76. ISSN: 0008-6223.

[43] Nur Laila Hamidah, Fu Ming Wang, and Gunawan Nugroho. "The understanding of solid electrolyte interface (SEI) formation and mechanism as the effect of flouro-o-phenylenedimaleimaide (F-MI) additive on lithium-ion battery". In: *Surface and Interface Analysis* 51.3 (2019), pp. 345–352.

[44] Christian Ekberg and Martina Petranikova. "Chapter 7 - Lithium Batteries Recycling". In: *Lithium Process Chemistry*. Ed. by Alexandre Chagnes and Jolanta Świątowska. Amsterdam: Elsevier, 2015, pp. 233–267. ISBN: 978-0-12-801417-2.

[45] Li-Po He et al. "Recovery of Lithium, Nickel, Cobalt, and Manganese from Spent Lithium-Ion Batteries Using l-Tartaric Acid as a Leachant". In: *ACS Sustainable Chemistry & Engineering* 5.1 (2017), pp. 714–721. DOI: 10.1021/acssuschemeng.6b02056.

[46] Tao Zhang et al. "Chemical and process mineralogical characterizations of spent lithium-ion batteries: An approach by multi-analytical techniques". In:

Waste Management 34.6 (2014). Waste Management on Asia, pp. 1051–1058. ISSN: 0956-053X.

[47] Yonglin Yao et al. "Hydrometallurgical Processes for Recycling Spent Lithium-Ion Batteries: A Critical Review". In: *ACS Sustainable Chemistry Engineering* 6 (Sept. 2018). DOI: 10.1021/acssuschemeng.8b03545.

[48] Tao Zhang et al. "Characteristics of wet and dry crushing methods in the recycling process of spent lithium-ion batteries". In: *Journal of Power Sources* 240 (2013), pp. 766–771. ISSN: 0378-7753.

[49] Yang Guo et al. "Leaching lithium from the anode electrode materials of spent lithium-ion batteries by hydrochloric acid (HCl)". In: *Waste Management* 51 (2016), pp. 227–233. ISSN: 0956-053X.

[50] Fathi Habashi. "Principles of Extractive Metallurgy". In: *Principles of Extractive Metallurgy* 1 (Jan. 1970), pp. 153–163.

[51] M. Joulié, R. Laucournet, and E. Billy. "Hydrometallurgical process for the recovery of high value metals from spent lithium nickel cobalt aluminum oxide based lithium-ion batteries". In: *Journal of Power Sources* 247 (2014), pp. 551–555. ISSN: 0378-7753.

[52] Supasan Sakultung, Kejvalee Pruksathorn, and Mali Hunsom. "Simultaneous recovery of valuable metals from spent mobile phone battery by an acid leaching process". In: *Korean Journal of Chemical Engineering* 24 (Jan. 2007), pp. 272–277. DOI: 10.1007/s11814-007-5040-1.

[53] Pratima Meshram et al. "Comparision of Different Reductants in Leaching of Spent Lithium Ion Batteries". In: *Journal of Metals* 68 (July 2016). DOI: 10.1007/s11837-016-2032-9.

[54] Liang Sun and Keqiang Qiu. "Vacuum pyrolysis and hydrometallurgical process for the recovery of valuable metals from spent lithium-ion batteries". In: *Journal of Hazardous Materials* 194 (2011), pp. 378–384. ISSN: 0304-3894.

[55] Rong-Chi Wang, Yu-Chuan Lin, and She-Huang Wu. "A novel recovery process of metal values from the cathode active materials of the lithium-ion secondary batteries". In: *Hydrometallurgy* 99.3 (2009), pp. 194–201. ISSN: 0304-386X.

[56] Liang Chen et al. "Process for the recovery of cobalt oxalate from spent lithium-ion batteries". In: *Hydrometallurgy* 108.1 (2011), pp. 80–86. ISSN: 0304-386X.

[57] Jeong-Soo Sohn et al. "Comparison of Two Acidic Leaching Processes for Selecting the Effective Recycle Process of Spent Lithium ion Battery". In: *Geosystem Engineering* 9 (Mar. 2006), pp. 1–6. DOI: 10.1080/12269328.2006.10541246.

[58] Manis Kumar Jha et al. "Recovery of lithium and cobalt from waste lithium ion batteries of mobile phone". In: *Waste Management* 33.9 (2013), pp. 1890–1897. ISSN: 0956-053X.

[59] Weiguang Lv et al. "A Critical Review and Analysis on the Recycling of Spent Lithium-Ion Batteries". In: *ACS Sustainable Chemistry & Engineering* 6.2 (2018), pp. 1504–1521. DOI: 10.1021/acssuschemeng.7b03811.

[60] Feng Wang et al. "Recovery of cobalt from spent lithium ion batteries using sulphuric acid leaching followed by solid-liquid separation and solvent extraction". In: *RSC Adv.* 6 (Sept. 2016). DOI: 10.1039/C6RA16801A.

[61] Pingwei Zhang et al. “Hydrometallurgical process for recovery of metal values from spent lithium-ion secondary batteries”. In: *Hydrometallurgy* 47.2 (1998), pp. 259–271. ISSN: 0304-386X.

[62] Sung-Ho Joo et al. “Extraction of manganese by alkyl monocarboxylic acid in a mixed extractant from a leaching solution of spent lithium-ion battery ternary cathodic material”. In: *Journal of Power Sources* 305 (2016), pp. 175–181. ISSN: 0378-7753.

[63] D. Darvishi et al. “Synergistic effect of Cyanex 272 and Cyanex 302 on separation of cobalt and nickel by D2EHPA”. In: *Hydrometallurgy* 77.3 (2005), pp. 227–238. ISSN: 0304-386X.

[64] Sung-Ho Joo et al. “Selective extraction and separation of nickel from cobalt, manganese and lithium in pre-treated leach liquors of ternary cathode material of spent lithium-ion batteries using synergism caused by Versatic 10 acid and LIX 84-I”. In: *Hydrometallurgy* 159 (2016), pp. 65–74. ISSN: 0304-386X.

[65] Sami Virolainen et al. “Solvent extraction fractionation of Li-ion battery leachate containing Li, Ni, and Co”. In: *Separation and Purification Technology* 179 (2017), pp. 274–282. ISSN: 1383-5866.

[66] Xiaoming Ma et al. “The Recycling of Spent Power Battery: Economic Benefits and Policy Suggestions”. In: *IOP Conference Series: Earth and Environmental Science* 159 (June 2018), p. 012017. DOI: 10.1088/1755-1315/159/1/012017.

[67] Wei-Sheng Chen and Hsing-Jung Ho. “Recovery of Valuable Metals from Lithium-Ion Batteries NMC Cathode Waste Materials by Hydrometallurgical Methods”. In: *Metals - Open Access Metallurgy Journal* 8 (May 2018). DOI: 10.3390/met8050321.

[68] Shun Myung Shin et al. “Development of a metal recovery process from Li-ion battery wastes”. In: *Hydrometallurgy* 79.3 (2005), pp. 172–181. ISSN: 0304-386X.

[69] Chao Peng et al. “Selective reductive leaching of cobalt and lithium from industrially crushed waste Li-ion batteries in sulfuric acid system”. In: *Waste Management* 76 (2018), pp. 582–590. ISSN: 0956-053X.

[70] Jack Schubert et al. “Catalytic decomposition of hydrogen peroxide by copper chelates and mixed ligand complexes of histamine in the presence of phosphate buffer in the neutral pH region”. In: *Journal of the American Chemical Society* 90.16 (1968), pp. 4476–4478.

A

Appendix 1

A.1 Calculation to find limiting reagent of the reaction at the condition of solid-to-liquid ratio of 1:10 g/ml

A purpose of these calculations is to examine whether the reaction is limited by the leaching solution, sulfuric acid used, or not when there is an absence of a reducing agent, H_2O_2. An example of calculation is shown below.

Example of calculation

Leaching of LCO, 1 g of solid and 10 ml of 2 M H_2SO_4 (solid-to-liquid ratio of 1:10)
Molecular weight of H_2SO_4 = 98.079 g/mol
Molecular weight of LCO = 97.87 g/mol

$$\text{Added amount of } H_2SO_4 = 10 \cdot 10^{-3} L \cdot \frac{2mol}{L} \cdot \frac{98.079g}{mol} = 1.962g \tag{A.1}$$

According to the leaching equation without H_2O_2

$$LiCoO_2(s) + 1.5H_2SO_4(aq) \rightleftharpoons CoSO_4(aq) + 0.5Li_2SO_4(aq) + 0.25H_2O(l) + 1.5O_2(g) \tag{A.2}$$

1 mol of LCO reacts with 1.5 mol of H_2SO_4

Theoretical amount of LCO needed = 97.87 g
Theoretical amount of H_2SO_4 needed = $1.5 \cdot 98.079g/mol$ = 147.112 g
The ratios between the added amount and theoretical amount needed for cathode material and H_2SO_4, which are referred to the number of times that each substance can actually react with the other, are calculated below.

$$\left(\frac{\text{Added amount}}{\text{Theoretical amount needed}}\right)_{LCO} = \frac{1g}{97.87g} = 1.02 \cdot 10^{-2} \tag{A.3}$$

$$\left(\frac{\text{Added amount}}{\text{Theoretical amount needed}}\right)_{H_2SO_4} = \frac{1.962g}{147.112g} = 1.33 \cdot 10^{-2} \tag{A.4}$$

It means that LCO can react with H_2SO_4 $1.02 \cdot 10^{-2}$ and will be used up before a running out of H_2SO_4 since its ratio is smaller. Therefore, LCO is limiting reagent and H_2SO_4 is excess reactant.

A.1.1 LCO

	$4LiCoO_2$	$+6H_2SO_4$	$\rightleftharpoons 4CoSO_4(\text{aq})+2Li_2SO_4(\text{aq})$ $+6H_2O(\text{l})+O_2(\text{g})$
M (g/mol)	97.87	98.079	
Added amount (g)	1	1.96158	
n (mol)		0.02	
c (mol/L)		2	
V (ml)		10	
Stoichiometric coef.	1	1.5	
Theo. amount (g)	97.87	147.12	
Added/Theo. amount	1.02×10^{-2}	1.33×10^{-2}	

LCO is limiting reagent and H_2SO_4 is excess reactant.

A.1.2 NMC111

	$12LiNi_{0.33}Mn_{0.33}Co_{0.33}O_2$	$+18H_2SO_4$	$\rightleftharpoons 4NiSo_4 + 4CoSO_4(aq)$ $+4MnSo_4 + 6Li_2SO_4(aq)$ $+18H_2O(l) + 3O_2(g)$
M (g/mol)	95.89	98.079	
Added amount (g)	1	1.96158	
n (mol)		0.02	
c (mol/L)		2	
V (ml)		10	
Stoichiometric coef.	12	18	
Theo. amount (g)	1150.65	1765.42	
Added/Theo. amount	8.7×10^{-4}	1.11×10^{-3}	

Therefore, NMC111 is limiting reagent and H_2SO_4 is excess reactant.

A.1.3 NMC622

	$20LiNi_{0.6}Mn_{0.2}Co_{0.2}O_2$	$+30H_2SO_4$	$\rightleftharpoons 12NiSo_4 + 4CoSO_4(aq)$ $+4MnSo_4 + 10Li_2SO_4(aq)$ $+30H_2O(l) + 5O_2(g)$
M (g/mol)	96.9313	98.079	
Added amount (g)	1	1.96158	
n (mol)		0.02	
c (mol/L		2	
V (ml)		10	
Stoichiometric coef.	20	30	
Theo. amount (g)	1938.6	2942.4	
Added/Theo. amount	5.16×10^{-4}	6.67×10^{-4}	

NMC622 is limiting reagent and H_2SO_4 is excess reactant.

A.1.4 NMC811

$$20LiNi_{0.8}Mn_{0.1}Co_{0.1}O_2 + 30H_2SO_4 \rightleftharpoons 16NiSo_4 + 2CoSO_4(aq) + 2MnSo_4 + 10Li_2SO_4(aq) + 30H_2O(l) + 5O_2(g)$$

M (g/mol)	97.28	98.079
Added amount (g)	1	1.96158
n (mol)		0.02
c (mol/L)		2
V (ml)		10
Stoichiometric coef.	20	30
Theo. amount (g)	1945.6	2942.4
Added/Theo. amount	5.14×10^{-4}	6.67×10^{-4}

NMC811 is limiting reagent and H_2SO_4 is excess reactant.

A.2 Calculation of theoretical hydrogen peroxide needed at the condition of solid-to-liquid ratio of 1:20 g/ml

Example of calculation
Leaching of LCO, 0.5 g of solid and 10 ml of 2 M H_2SO_4
Molecular weight of H_2SO_4 = 98.079 g/mol
Molecular weight of LCO = 97.87 g/mol
Molecular weight of H_2O_2 = 34.016 g/mol

Density of H_2O_2 (59w/w%) = 1.241 g/cm^3
Concentration of concentrated H_2O_2 (59w/w%) is calculated below.

$$\text{H}_2\text{O}_2 \text{ conc.} = Density \cdot \%weight = \frac{1.241g}{cm^3} \cdot \frac{59gH_2O_2}{100gsolution} \cdot \frac{1cm^3}{0.001L} = 732.19g/L \tag{A.5}$$

$$\text{Number of mole (cathode material)} = \frac{\text{Cathode material weight (g)}}{\text{Molecular weight of cathode material (g/mol)}} \tag{A.6}$$

$$\text{Number of mole (LCO)} = 0.5g \cdot \frac{mol}{97.87g} = 5.11 \cdot 10^{-3}mol \tag{A.7}$$

According to its leaching equation with H_2O_2 as shown below:

$$2LiCoO_2 + 3H_2SO_4 + H_2O_2 \rightleftharpoons 2CoSO_4 + Li_2SO_4 + 4H_2O + O_2 \quad \text{(A.8)}$$

Thus, 2 mol of LCO will react perfectly with 1 mol of H_2O_2.

$$\text{Number of } H_2O_2 \text{ mole} = \frac{5.11 \cdot 10^{-3} mol}{2} = 2.55 \cdot 10^{-3} mol \quad \text{(A.9)}$$

$$H_2O_2 \text{ weight} = 2.55 \cdot 10^{-3} mol \cdot \frac{34.015 g}{mol} = 0.087 g \quad \text{(A.10)}$$

$$\text{Volume of } H_2O_2 \text{ needed} = 0.087 g \cdot \frac{1000 ml}{732.19 g} = 0.119 ml \quad \text{(A.11)}$$

0.119 ml of H_2O_2 (1.19vol%) is needed to leach LCO with H_2SO_4 at the solid-to-liquid ratio of 1:20 g/ml.

Based on the above H_2O_2 volume needed, the concentration in the unit of g/L is calculated below.

Volume of H_2O_2 in 10 mL solution = 0.119 mL

$$H_2O_2 \text{ conc.} = \frac{C_{concentrated} \cdot V_{concentrated}}{V_{solution}} = \frac{732.19 g/L \cdot 0.119 mL}{10 mL} = 8.7 g/L \quad \text{(A.12)}$$

Therefore, 8.7 g/L of H_2O_2 is needed theoretically to leach LCO with H_2SO_4 at the solid-to-liquid ratio of 1:20 g/ml.

A.2.1 LCO

	$2LiCoO_2$	$+3H_2SO_4$	$+H_2O_2$
M (g/mol)	97.87	98.079	34.016
Weight (g)	0.5	1.96158	0.087
n (mol)	5.11×10^{-3}	0.02	2.55×10^{-3}
c (mol/L)		2	
V (ml)		10	0.119
c (g/L)			8.71

1.19vol% (8.7 g/L) of H_2O_2 is needed to leach LCO with H_2SO_4 at the solid-to-liquid ratio of 1:20 g/ml.

A.2.2 NMC111

	$6LiNi_{0.33}Mn_{0.33}Co_{0.33}O_2$	$+9H_2SO_4$	$+H_2O_2$
M (g/mol)	95.8872	98.079	34.016
Weight (g)	0.5	1.96158	0.0295
n (mol)	5.21×10^{-3}	0.02	8.68×10^{-4}
c (mol/L)		2	
V (ml)		10	0.04
c (g/L)			2.93

0.40vol% (2.9 g/L) of H_2O_2 is needed to leach NMC111 with H_2SO_4 at the solid-to-liquid ratio of 1:20 g/ml.

A.2.3 NMC622

	$10LiNi_{0.6}Mn_{0.2}Co_{0.2}O_2$	$+15H_2SO_4$	$+H_2O_2$
M (g/mol)	96.9313	98.079	34.016
Weight (g)	0.5	1.96158	0.0176
n (mol)	5.16×10^{-3}	0.02	5.16×10^{-4}
c (mol/L)		2	
V (ml)		10	0.024
c (g/L)			1.76

0.24vol% (1.76 g/L) of H_2O_2 is needed to leach NMC622 with H_2SO_4 at the solid-to-liquid ratio of 1:20 g/ml.

A.2.4 NMC811

	$40LiNi_{0.8}Mn_{0.1}Co_{0.1}O_2$	$+60H_2SO_4$	$+2H_2O_2$
M (g/mol)	97.2828	98.079	34.016
Weight (g)	0.5	1.96158	8.74×10^{-3}
n (mol)	5.14×10^{-3}	0.02	2.57×10^{-4}
c (mol/L)		2	
V (ml)		10	0.012
c (g/L)			0.87

0.12vol% (0.87 g/L) of H_2O_2 is needed to leach NMC811 with H_2SO_4 at the solid-to-liquid ratio of 1:20 g/ml.